INTERACTIVE CONTROL ENGINEERING
Principles and Applications

Volume 17 Control of Energy Conversion and Storage

CHAPTER 9

Electric Vehicle Fast Charge Simulator for Selector Control of an Unmeasured Constraint

Pages 218–247

Edited by John D. Hedengren

How to cite this chapter. "Electric Vehicle Fast Charge Simulator for Selector Control of an Unmeasured Constraint," in *Control of Energy Conversion and Storage*, John D. Hedengren, Ed., vol. 17 of *Interactive Control Engineering: Principles and Applications*. Advanced Process Solutions, LLC, 2026, ch. 9, pp. 218–247.

The page numbers in this file are those of the printed volume.

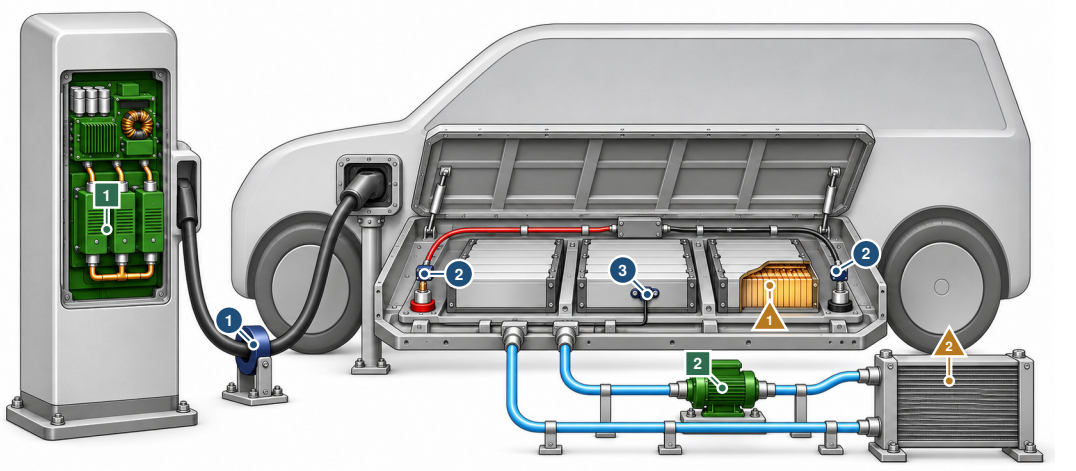
The app for this chapter
https://apmonitor.com/apps/ev-fast-charge/

The volume online: contents, other chapters and citation records
https://apmonitor.com/apps/books/v17-energy/#ev-fast-charge

Copyright © 2026 Advanced Process Solutions, LLC. All rights reserved. Produced by Advanced Process Solutions, LLC.

CHAPTER 9

Electric Vehicle Fast Charge Simulator for Selector Control of an Unmeasured Constraint



The controller moves 1 charger power stages that set the current 2 coolant pump

The controller reads 1 current sensor on the cable 2 voltage taps at the pack terminals 3 thermistor on a module case

What disturbs it 1 cell aging the stored table does not know 2 ambient air at the chiller

Notice that every sensor sits outside the cells, while the limit that ends the charge lies at the graphite surface inside them. Illustration, not to scale.

IN PLAIN TERMS **Charging Fast Without Hurting the Battery**

The main idea. A fast charger pushes current into a car's battery as fast as the battery can safely take it. The real limit is a tiny voltage at the carbon surface inside each cell, and no sensor in the car can read it.

The challenge. So the car works it out from a stored table and a few gauges, and keeps a safety gap. If the table is wrong, as it becomes when the battery ages, lithium metal coats the carbon while every gauge looks normal.

Why it matters. Each such charge quietly takes away some of the battery's driving range for good.

THREE WAYS TO READ THIS CHAPTER

Explore	11 min	The first page, the history box of Section 9.2, the fact box of Section 9.3, the try-it and fact boxes of Section 9.6, and the key points
Study	60 min	The whole chapter with its pause points and the twelve exercises
Practice	25 min	The first page, Section 9.6, Section 9.7, Section 9.8 and the open challenges

The control question Four limits share one charging current, and the one that ends a fast charge, the anode surface potential, has no instrument. How should a selector defend a constraint it can only compute, and what margin does an error in that computation cost?

Learning objectives

- Compute the anode-limited current from the plateau potential and the kinetic resistance at a state of charge and temperature.
- Explain why the anode limit is an inverse map that cannot be given integral action.
- Size the anode margin as a budget for kinetic table error.
- Explain how external reset and a capped preload keep a low selector from ratcheting its output down.
- Compare the selector with a predictive controller on time, peak core temperature and plated lithium.

Prerequisites Sections 1.4.4 (storage state and tapered limits), 1.4.7 (a limit or selector joining the layers), 1.6.2 (velocity form, external reset), 1.6.3 (predictive control, Kalman filter) and 1.6.4 (scenarios and data).

The app https://apmonitor.com/apps/ev-fast-charge/

See also Volume 4, Chapter 3 for a min/max selector over limiters guarding a surge margin no sensor reads, and Volume 4, Chapter 2 for a protective override that rests on its clamp. Volume 5, Chapter 11 and Volume 5, Chapter 10 for control of a temperature and a constraint that are inferred rather than measured.

9.1 Introduction

A constraint in an introductory control problem arrives with an instrument behind it. A pressure has a transmitter, a level has a float, a metal temperature has a thermocouple welded to it, and the controller that defends the constraint acts on the difference between what the instrument reports and where the limit was drawn. Charging a lithium-ion vehicle pack breaks that arrangement at the only point where it matters. Three of the four limits on the charging current are instrumented, being the rating of the charging post, the terminal voltage of the pack and the cell temperature, and not one of the three is what ends a fast charge. What ends it is the electric potential of the graphite surface against lithium metal, and no vehicle in service carries a reference electrode that reports it [1].

That potential decides the chemistry. Lithium arriving at the negative electrode intercalates into the graphite while the surface stays above the potential of lithium metal, and below that value it deposits as metal on the surface instead [2]. Part of the deposit never rejoins the inventory, and what remains is a rough surface that deposits more readily on the next charge [3], with the simulator treating 62 % of it as permanently lost. The equilibrium potential of graphite falls onto a low plateau over most of its range of lithiation [4], taken here as 85 mV, so the whole margin available to a fast charge is a few tens of millivolts of overpotential, and the overpotential is the charging current multiplied by a kinetic resistance that rises steeply as the electrode fills and as the cell cools [5].

A block diagram of this plant has a comparator drawn in front of the anode controller, and drawing it is the mistake. What the application corrects is the belief that a limit is defended as soon as a setpoint has been written for it. A feedback loop is wrong by the amount its plant departs from its setpoint, and the error signal that measures the departure is the same signal that removes it. An inverse model carries no such signal. It is wrong by the amount the model departs from the plant, that discrepancy appears nowhere in the instrument set, and integral action cannot be added because there is no error to integrate. The application shows the two side by side on one screen, with the computed anode potential that a vehicle would display drawn against the true anode potential that a vehicle cannot obtain, and the distance between the two lines is the subject of this chapter.

The class of problem is constraint control on an inferred variable that shares an actuator with measured constraints, resolved by a selector, and it is general. Selective and override schemes are the standard answer wherever several limits compete for one handle, and the losing controllers have to be told what was actually applied or their integrals will wind up while they are out of service [6, 7]. Battery management is a well-documented instance of the same structure [8], and the shape recurs

whenever the binding quantity sits somewhere an instrument cannot go, such as a metal temperature inside a casting, a film boiling point on the inside of a tube, or a stress at a weld root. The core of a brick in the cathode kiln of Volume 5, Chapter 11 is another such place. In each case the constraint enters the selector as a computed number, stands beside constraints that do have transmitters, and is protected by a margin that somebody has to justify to a design review.

This chapter makes three kinds of statement. The first is a measurement rather than a method, a controlled comparison on one pack between a constant-current charge and an anode-limited charge that reports the four and a half minutes the second one costs alongside the 3.381 Ah of plated lithium the first one produces, and a sweep of the constraint margin against kinetic model error that turns the margin into a budget with numbers in it. The second is a nine-state electrochemical, thermal and aging model with a four-way low selector, written out below in enough detail to be rebuilt from the text. It runs in a browser at interactive speed beside an optional model predictive controller that is measured against the selector on seven cases. The third is the scenario set and the manual mode underneath it, where the plating threshold is found by pushing current into the pack and watching a line that a real vehicle does not have. Neither the cell model nor the selector arithmetic is new. The aim is to write down a fast charge whose binding limit is computed instead of measured, and to price what that substitution costs when the computation is wrong.

Section 9.2 follows the domain from constant-current charging to the charge current limit map. Section 9.3 states the plant, its parameters and its assumptions. Section 9.4 reads the four limits as functions of the operating point, and Section 9.5 gives the implemented scheme: the shared PID routine, the anode map, the selector with its preload and the predictive alternative. Section 9.6 carries the measured scenarios, Section 9.7 describes the hardware of a real vehicle and charger, Section 9.8 states what the model cannot support, Section 9.9 draws the lessons that carry beyond batteries and Section 9.10 collects the main numbers.

9.2 From Constant Current to a Charge Current Limit Map

The protocol that lithium-ion cells inherited is constant current followed by constant voltage. Current is held at a rate the cell vendor guarantees until the terminal voltage reaches its ceiling, and the voltage is then held while the current decays. Both numbers come from a data sheet rather than from the state of the cell, which is why the protocol is safe at a third of a C and unsafe at two, and why the first serious studies of fast charging were comparisons of protocols on cycle life rather than analyses of any mechanism. Cells charged to the same terminal voltage by different current histories were shown to lose capacity at markedly different rates, with the loss traced to the negative electrode rather than to the positive [9]. Pulse and boost protocols were proposed on the reasoning that a resting interval lets concentration gradients relax and raises the surface potential before the next pulse [10], which is a correct mechanism attacked without a measurement of the quantity it acts on.

The quantity itself was available in the modeling literature well before it reached a vehicle. The porous-electrode formulation of the lithium insertion cell resolves solid-phase and electrolyte concentrations and returns the local electrode potential at every point through the thickness [11], and a deposition side reaction was added to that framework with a criterion for the onset of metallic lithium expressed directly as the potential of the solid surface against a lithium reference [2]. The equilibrium half of that potential had been measured for graphite over its whole range of lithiation, with the staging plateaus that produce the flat region a fast charge has to work inside [4]. Low-temperature work then established the part that surprises drivers, that a cold cell is slow because the intercalation kinetics are slow rather than because a controller is being cautious [5], and a later review collected the evidence that plating is partly irreversible and that its consequences are morphological as well as coulombic [3].

Control formulations followed once the criterion existed. The estimation and control problems specific to a pack were set out as a class, with the observation that the quantities a management system would most like to bound are internal states rather than terminal measurements [8], and a charging

problem was then posed explicitly as maximizing the charge delivered subject to a lower bound on the computed side-reaction overpotential rather than to an upper bound on the terminal voltage [12]. Later work carried the formulation into a coupled electro-thermal-aging setting and traded the charge time against the predicted capacity loss in one objective [13]. Production practice took a simpler route than an on-line optimizer. The solution shipped in vehicles is a charge current limit map, a table of allowable current against state of charge and temperature computed offline from the same criterion, looked up every scan and passed to a selector alongside the voltage and temperature limits, and it is the reason a modern charge curve tapers continuously from the moment the charger ceiling is released. Reviews of fast charging from the end of the last decade describe the limit map as the standard answer and identify its weakness, which is that the table is fitted to particular cells at a particular age [14], and the same weakness appears in technology gap assessments alongside the thermal and infrastructure constraints on a ten to eighty percent charge in fifteen minutes [15]. Closing that gap by measurement rather than by margin is an active subject, with adaptive schemes that identify a virtual reference electrode on line and control the anode potential against it directly [1]. The application in this chapter implements the standard answer and the failures that motivate the adaptive one.

> ⧖ HISTORY **A Ten-Minute Target for Fast Charging (2017)**
>
> In 2017 a group of United States national laboratories assessed what it would take to recharge an electric vehicle about as quickly as a car is refueled. Direct-current fast chargers then on the market delivered up to 120 kW, and the assessment defined extreme fast charging as recharging up to 80 % of the battery capacity in 10 min or less [15]. Most packs of the day were rated at or below 400 V, and the companion vehicle study set 800 to 1000 V and more than 400 kW as the design point for future vehicles [16]. The assessment also warned that the conventional constant-current, constant-voltage protocol may not suit such charging, because of the high probability of lithium plating toward the end of the charge [15].

9.3 Pack and Cell Model

The simulated vehicle carries 96 cells in series of 200 Ah each, which is 316.8 V at the empty end of the open-circuit curve and 398.4 V at the full end, and 49.7 kWh of stored energy between 10 and 80 % state of charge. The post is rated 250 kW and the vehicle contactors are rated 500 A, which at these terminal voltages is 165 to 199 kW, so the current ceiling binds on this pack and the power rating never does. A liquid loop carries heat from the pack to a chiller whose capacity falls with ambient temperature. All of that appears in Figure 9.1, together with the instruments, the block that computes the anode potential and every symbol carried into the equations of this section.

The clock runs in minutes because a charge takes 17 to 45 of them. Currents are in amperes, voltages in volts, temperatures in degrees Celsius with the Arrhenius terms converted to kelvin internally, heat rates in kilowatts and charge in ampere hours. State of charge is a fraction in the equations and is displayed as a percentage.

9.3.1 Variables

Everything the application exposes is classified in Table 9.1. The single manipulated variable that matters is the charging current, and four candidate controllers write to it. The coolant flow is a second manipulated variable belonging to a loop of its own.

9.3.2 The Cell as a Circuit

Terminal behavior is an open-circuit curve, two polarization branches and an ohmic drop, as shown in Equation (9.1).

$$\begin{aligned} V &= n_s U_{ocv}(z) + v_1 + v_2 + I R_0(T) \\ \frac{\mathrm{d}v_k}{\mathrm{d}t} &= \frac{60\,(I R_k - v_k)}{R_k C_k}, \qquad k = 1,2 \end{aligned} \tag{9.1}$$

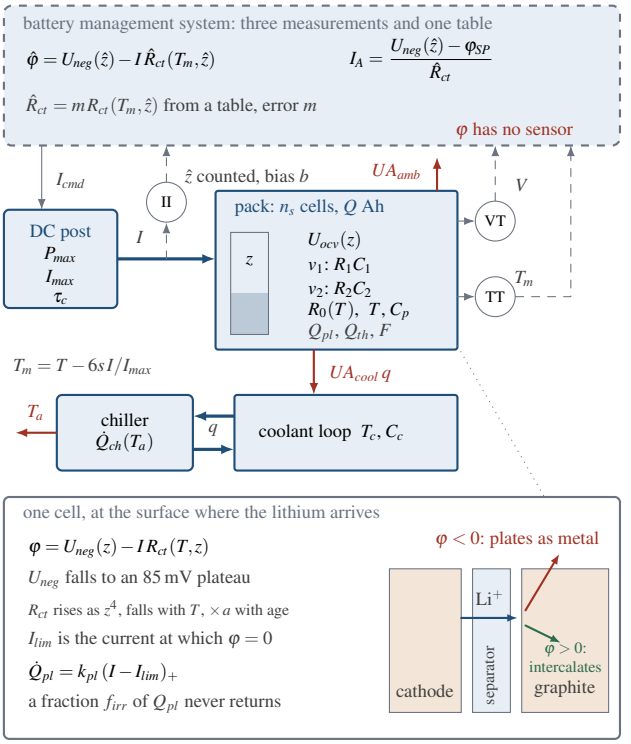


Figure 9.1 Vehicle pack on a direct-current post, with the coolant loop beneath it and the cell surface enlarged below. The management system reads the pack current, the terminal voltage V and one thermistor T_m on the module case, counts the state of charge as $\hat{z}$, and computes the anode surface potential $\hat{\varphi}$ from a kinetic table carrying error m. Solid heavy lines are power, dashed lines are signals, and the short thick arrows labeled with a conductance or the ambient temperature are heat. Nothing in the vehicle measures φ.

where n_s is the series count, v_k is the voltage across branch k of the pack in volts, R_k and C_k are that branch resistance and capacitance, and the factor 60 converts the branch time constant from seconds to minutes. The open-circuit curve carries a steep tail and a low-state-of-charge knee, as shown in Equation (9.2).

$$U_{ocv}(z) = 3.30 + 0.55z + 0.15z^8 + 0.15\left(1 - \mathrm{e}^{-20z}\right) \tag{9.2}$$

in volts per cell, giving 3.30 V empty, 3.73 V at half charge and 4.15 V full. Every resistance in the pack is Arrhenius in temperature and grows together with cell age, as shown in Equation (9.3).

$$R_j(T) = R_j^0\, a \exp\left[E_R\left(\frac{1}{T_K} - \frac{1}{T_{ref}}\right)\right], \quad j = 0,1,2 \tag{9.3}$$

where $T_K = T + 273.15\,\mathrm{K}$ is the absolute pack temperature, $T_{ref} = 298.15\,\mathrm{K}$, E_R is an activation temperature in kelvin and a is the aging multiplier. Equation (9.3) is why a cold pack is a resistive pack and a resistive pack is a hot pack, and 500 A through the nominal 23.5 mΩ deposits 5.88 kW in the cells, which is the same order as the chiller.

9.3.3 The Potential That Decides the Chemistry

The quantity the whole application is built around is the potential of the graphite surface against lithium metal, and it is the equilibrium potential of the electrode less the overpotential the current has

Table 9.1 Variable classification. Ranges are the limits the application enforces on a slider or a state.

Symbol	Meaning	Unit	Range
Constrained and controlled variables			
φ	anode surface potential, true	mV	not measured
$\hat{\varphi}$	anode potential, as computed	mV	SP 0 to 80
V	pack terminal voltage	V	limit $n_s V_{max}$
T	pack core temperature	°C	derate SP 30 to 55
z	state of charge	%	target 50 to 100
Manipulated variables			
I_{cmd}	charging current command	A	0 to 500
q	coolant flow	%	0 to 100
Disturbances and the post rating			
T_a	ambient temperature	°C	−15 to 45
m	kinetic table error	×	0.50 to 1.60
a	cell aging multiplier	×	1.00 to 2.20
s	thermistor offset scale	×	0 to 2
b	current sensor error	×	0.950 to 1.050
P_{sp}	power the post offers	kW	20 to 400
States			
z	state of charge	—	0 to 1.02
v_1, v_2	polarization voltages	V	≥ 0
T	pack core temperature	°C	−30 to 90
T_c	coolant temperature	°C	unbounded
I	current flowing	A	0 to I_{max}
Q_{pl}	plated lithium	Ah	≥ 0
Q_{th}	charge throughput	Ah	≥ 0
F	capacity fade	%	0 to 40
Measurements			
$\hat{z}$	counted state of charge	%	0 to 105
$\hat{V}$	filtered terminal voltage	V	—
T_m	thermistor on the case	°C	—

to drive through the intercalation kinetics, as shown in Equation (9.4).

$$\varphi = U_{neg}(z) - I R_{ct}(T,z), \qquad U_{neg}(z) = U_0 + U_A \mathrm{e}^{-k_U z} \tag{9.4}$$

where φ is in volts, U_0 is the plateau potential of lithiated graphite, U_A is the rise on an empty electrode and k_U sets how quickly that rise decays. Equation (9.4) returns 685 mV on an empty anode, 266 mV at 10 % and 85.4 mV at 60 %, so the margin available for the overpotential collapses within the first tenth of a charge. The kinetic resistance is Arrhenius in temperature and rises as the fourth power of lithiation, as shown in Equation (9.5).

$$R_{ct}(T,z) = R_{ct}^{0}\, a \left(1 + k_R z^4\right) \exp\left[E_c \left(\frac{1}{T_K} - \frac{1}{T_{ref}}\right)\right] \tag{9.5}$$

where E_c is the activation temperature of the anode kinetics and k_R sets how steeply the resistance grows as the electrode fills. Setting $\varphi = 0$ in (9.4) gives the plating current, and setting φ to any target margin gives the current a controller would allow, as shown in Equation (9.6).

$$I_{lim}(T,z) = \frac{U_{neg}(z)}{R_{ct}(T,z)}, \qquad I(\varphi^*) = \frac{U_{neg}(z) - \varphi^*}{R_{ct}(T,z)} \tag{9.6}$$

Equation (9.6) is the whole control problem in one line, because it is an algebraic inverse of the model rather than a measurement of anything, and its right-hand side is built from a state of charge

that was counted, a temperature read some distance from the reaction and a resistance taken from a table.

Current beyond I_{lim} deposits metal, and a fixed fraction of the deposit is treated as permanently lost, as shown in Equation (9.7).

$$\frac{\mathrm{d}Q_{pl}}{\mathrm{d}t} = \frac{k_{pl}}{60}\,(I - I_{lim})_{+} \tag{9.7}$$

where $(\cdot)_{+}$ is the positive part, k_{pl} is the fraction of the excess current that plates and the factor $1/60$ converts amperes to ampere hours per minute. Capacity fade accumulates from throughput with an Arrhenius temperature factor and from the irreversible part of the deposit, as shown in Equation (9.8).

$$\frac{\mathrm{d}F}{\mathrm{d}t} = \frac{k_{cyc} I}{60} \exp\left[E_f\left(\frac{1}{T_{ref}} - \frac{1}{T_K}\right)\right] + k_{pf} f_{irr} \frac{\mathrm{d}Q_{pl}}{\mathrm{d}t} \tag{9.8}$$

where F is in percent of nameplate capacity, k_{cyc} is the fade per ampere hour at 25 °C, E_f is the activation temperature of throughput aging, f_{irr} is the irreversible fraction of the plated lithium and k_{pf} is the fade per ampere hour of it. The two terms in (9.8) have very different characters. Throughput aging is slow and unavoidable, while the plating term can produce more damage in the last three minutes of one charge than the first term produces in the whole of it.

Coulomb counting closes the state of charge on the effective capacity, as shown in Equation (9.9).

$$\frac{\mathrm{d}z}{\mathrm{d}t} = \frac{I}{60\,Q\,(1 - F/100)}, \qquad \frac{\mathrm{d}Q_{th}}{\mathrm{d}t} = \frac{I}{60} \tag{9.9}$$

with Q in ampere hours and z dimensionless.

9.3.4 Thermal Side and the Chiller

Two thermal nodes are integrated, the pack and the coolant leaving the chiller, as shown in Equations (9.10) and (9.11).

$$\frac{\mathrm{d}T}{\mathrm{d}t} = \frac{60}{C_p}\left[\dot{Q}_{gen} - UA_{cool}\,\tfrac{q}{100}(T - T_c) - UA_{amb}(T - T_a)\right] \tag{9.10}$$

$$\frac{\mathrm{d}T_c}{\mathrm{d}t} = \frac{60}{C_c}\left[UA_{cool}\,\tfrac{q}{100}(T - T_c) - \dot{Q}_{ch} + UA_{cl}(T_a - T_c)\right] \tag{9.11}$$

where C_p and C_c are heat capacities in kJ/°C, the conductances are in kW/°C, q is the coolant flow in percent and the factor 60 converts kW/(kJ °C) to degrees per minute. Loss heat is ohmic plus polarization, as shown in Equation (9.12).

$$\dot{Q}_{gen} = \frac{1}{1000}\left(I^2 R_0 + \frac{v_1^2}{R_1} + \frac{v_2^2}{R_2}\right) \tag{9.12}$$

in kilowatts with the resistances in ohms. The chiller runs only while current is flowing and its capacity falls linearly with ambient temperature, as shown in Equation (9.13).

$$\dot{Q}_{ch} = \mathbb{1}[I_{cmd} > 2\,\mathrm{A}]\,\mathrm{clip}\big(k_{ch}(T_c - T_c^{set}),\ 0,\ \dot{Q}_{ch}^{max}\big) \tag{9.13}$$

with $\dot{Q}_{ch}^{max} = \max\big[0,\ \dot{Q}_0\,(1 - f_{ch}(T_a - 25))\big]$, where $\dot{Q}_0$ is the capacity at 25 °C and f_{ch} is the fractional loss per degree. The indicator function in (9.13) is why a parked pack sits at ambient rather than being quietly refrigerated, and it is what makes the resting scenario a genuine equilibrium.

> **DID YOU KNOW? The Heat of a Ten-Minute Charge**
>
> A 2017 thermal study of a 66 kWh pack on a 350 kW charger put the pack's heat generation at 39 to 116 kW, for charge efficiencies of 90 down to 70 %. It called a 15 kW cooling system substantially oversized compared with most vehicles then on the market [17].

9.3.5 Charger, Instruments and the Counted State of Charge

The post is a current source with a first-order response, as shown in Equation (9.14).

$$\frac{\mathrm{d}I}{\mathrm{d}t} = \frac{I_{cmd} - I}{\tau_c} \tag{9.14}$$

with τ_c in minutes. Three signals reach the controller. The thermistor sits on the module case rather than in the jelly roll, so it reads low while the current is high, and it is filtered, as shown in Equation (9.15).

$$\begin{aligned} T_m^k &= \alpha_T T_m^{k-1} + (1-\alpha_T)\left(T - 6\,s\,\frac{I}{I_{max}}\right) \\ \alpha_T &= \mathrm{e}^{-\Delta t_c/\tau_{Tm}} \end{aligned} \tag{9.15}$$

where s is the offset scale, the constant 6 °C is the full-current gap at $s = 1$ and Δt_c is the controller period. The terminal voltage passes through the same exact zero-order-hold update with time constant τ_{Vm}. State of charge is counted from the current with whatever error the sensor carries, as shown in Equation (9.16).

$$\hat{z}_k = \hat{z}_{k-1} + \frac{b\,I\,\Delta t_c}{60\,Q} \tag{9.16}$$

where b is the current sensor error. Equation (9.16) uses the nameplate capacity rather than the faded capacity of (9.9), which is deliberate, because a vehicle counts against what it was told the pack holds.

Three different models are in play here, and confusing them is the usual error. The plant is Equations (9.1) to (9.14) with the true temperature T, the true state of charge z and the true aging multiplier a. The controller internal model is Equations (9.4), (9.5) and (9.6) evaluated at T_m, $\hat{z}$ and a table multiplier m in place of a, which is the map the management system actually carries. There is no identified control model, because nothing in the application fits a transfer function to data, and the gains in Section 9.5 are supplied rather than derived. The predictive strategy of Section 9.5.5 carries a second internal model, also written rather than identified, from the same equations at their declared values.

9.3.6 Parameters

Table 9.2 lists every constant the equations use. Three of them are hidden from the model panel and the rest are displayed and adjustable, which is a lighter concealment than the identification applications in this series use, because the problem here is structural rather than one of estimation. The post rating P_{max} caps the offered power P_{sp} of Table 9.1 in the charger candidate of Section 9.5, and at its 250 kW default it never binds on this pack.

9.3.7 Initialization and Numerics

A run opens with the state of charge and the pack temperature taken from two segmented controls, at 10, 30 or 55 % and at 0, 5, 15, 25, 35 or 38 °C. Both are read only at initialization, so a new arrival condition acts at once before a run and at the next Reset during one. Both polarization voltages, the current and the three counters open at zero, and the coolant starts at the pack temperature. The default arrival is 10 % and 25 °C. Four bounds are enforced after every step, with z clipped to 1.02, the current to I_{max}, the pack temperature to the range −30 to 90 °C and the fade to 40 %.

Table 9.2 Model parameters. Hidden constants are never displayed in the application.

Symbol	Meaning	Value	Unit	Visibility
n_s	cells in series	96	—	adjustable
Q	pack capacity	200	Ah	adjustable
R_0^0	ohmic resistance	0.0235	Ω	adjustable
R_1^0	charge-transfer branch	0.0090	Ω	adjustable
C_1	charge-transfer branch	2200	F	adjustable
R_2^0	diffusion branch	0.0055	Ω	adjustable
C_2	diffusion branch	42000	F	adjustable
E_R	activation, resistances	3600	K	adjustable
V_{max}	cell voltage limit	4.15	V	adjustable
U_0	graphite plateau	0.085	V	adjustable
U_A	rise on empty anode	0.60	V	adjustable
k_U	decay of that rise	12	—	adjustable
R_{ct}^0	kinetic resistance	1.2×10^{-4}	Ω	adjustable
k_R	lithiation coefficient	8.0	—	adjustable
E_c	activation, kinetics	4000	K	adjustable
k_{pl}	plated fraction of excess	0.55	—	adjustable
f_{irr}	irreversible fraction	0.62	—	adjustable
C_p	pack heat capacity	340	kJ/°C	adjustable
UA_{cool}	pack to coolant, full flow	1.55	kW/°C	adjustable
UA_{amb}	pack to cabin	0.09	kW/°C	adjustable
$\dot{Q}_0$	chiller at 25 °C	6.5	kW	adjustable
f_{ch}	capacity lost per degree	0.018	1/°C	adjustable
T_c^{set}	coldest coolant	15	°C	adjustable
T_{max}	cell temperature limit	45	°C	adjustable
k_{ch}	chiller control gain	1.4	kW/°C	hidden
C_c	coolant heat capacity	25	kJ/°C	hidden
UA_{cl}	coolant to ambient	0.05	kW/°C	hidden
I_{max}	vehicle current ceiling	500	A	adjustable
P_{max}	post power rating	250	kW	adjustable
τ_c	charger current response	0.02	min	adjustable
E_f	activation, throughput fade	5500	K	adjustable
k_{cyc}	fade per ampere hour	3.4×10^{-4}	%/Ah	adjustable
k_{pf}	fade per plated ampere hour	0.010	%/Ah	adjustable
τ_{Tm}	thermistor filter	0.25	min	adjustable
τ_{Vm}	voltage filter	0.02	min	adjustable

Each 0.005 min of simulated time, which is 0.3 s, is advanced by one classical Runge-Kutta step of fourth order, by the engine of Section 1.6.1. The management system executes on a 0.02 min period, which is 1.2 s and is a realistic scan for a pack controller, and the two sensor filters in (9.15) advance on that same period rather than on the physics step. The historian keeps one sample every 0.035 min, which is seven physics steps or 2.1 s. There is no stochastic term anywhere in this application, so every scenario is deterministic and the trends, the scorecard and the exported file are identical on any machine. Speed multipliers between 0.5 and 10 simulated minutes per wall second leave the trajectory untouched.

9.3.8 Assumptions

Six simplifications hold this model up, and the paragraph for each one names the condition that breaks it.

One equivalent cell, scaled to the pack. Series and parallel spread, balancing and the weakest cell are all absent. On a real pack the management system defends the weakest cell rather than the average one, and that cell is usually several percent away, so the margins reported here are optimistic by whatever the spread happens to be.

A lumped anode criterion rather than a porous electrode. The plateau potential and the lumped kinetic resistance of (9.4) and (9.5) reproduce the shapes that a distributed model gives [2, 11], which are a flat equilibrium region, an Arrhenius temperature dependence and a steep rise as the electrode fills, but there is no solid-phase diffusion, no exchange current density and no variation through the electrode thickness. The criterion therefore locates the onset of plating at one surface rather than at the separator face where a distributed model puts it first.

Plating is proportional to the overshoot with no threshold. Equation (9.7) starts depositing the instant φ crosses zero. Real deposition needs a nucleation overpotential, part of it strips back on rest, and the damage depends on morphology far more than on quantity [3]. Dendrite growth and separator penetration are outside the model entirely, so nothing here supports a statement about safety.

Two thermal nodes. There is no gradient inside a module, no cell-to-coolant film and no cold plate, and pack thermal design is largely about those three. The 6 °C core-to-case gap in (9.15) is a fitted offset proportional to current rather than a conduction path, so it responds instantly to a current change where a real gradient would lag.

Two aging terms. Calendar aging, depth of discharge, resting state of charge and the interactions among them are absent from (9.8), so a projection over five hundred charges illustrates a mechanism and does not predict a life. The ratios between strategies are the usable result and the absolute percentages are the arithmetic of this model.

The post is a current source with a ceiling. Real direct-current chargers run control loops of their own, negotiate continuously with the vehicle, derate on cable temperature and time out on communication faults. Here the post follows (9.14) with one time constant and a power limit.

9.4 The Constraint Surface

Before any controller is discussed it is worth reading the four limits as functions of the operating point, because the answer decides which of them is worth tuning. Figure 9.2 plots the anode-limited and voltage-limited currents against state of charge, with the two measured charge trajectories drawn over them.

Three readings follow from Figure 9.2. The anode limit is below the voltage limit everywhere on the working range, by a factor of 3.6 at half charge (480 A against 1734 A) and 5.8 at 80 % (166 A against 959 A), so a charge that respects the terminal voltage and nothing else is not protected at all. Among the four, the anode limit alone is a strong function of what the operator is doing, because it moves with both the state of charge the current is creating and the temperature the current is generating, while the charger rating and the cell voltage limit are properties of the equipment. Cold makes it worse by the amount (9.5) predicts, since the kinetic resistance at 0 °C is 3.41 times its value at 25 °C and the allowable current at half charge falls from 480 to 141 A.

The consequence for a charge curve is the shape drawn solid with circles. The charger ceiling holds the current for the first part of the charge, the anode limit descends through it, and from that crossing the current follows a continuous taper set by an electrode potential rather than a step change set by a voltage limit. The classical constant-voltage phase all but disappears on this pack once the anode is represented (on the charge to a hundred percent of scenario 10 the terminal voltage reaches its limit only at 98.4 % true charge and holds the current for the last 4.6 min), which is worth stating plainly, because the constant-voltage phase on a real charge curve is largely what a voltage loop does when it is standing in for a constraint that was never modeled.

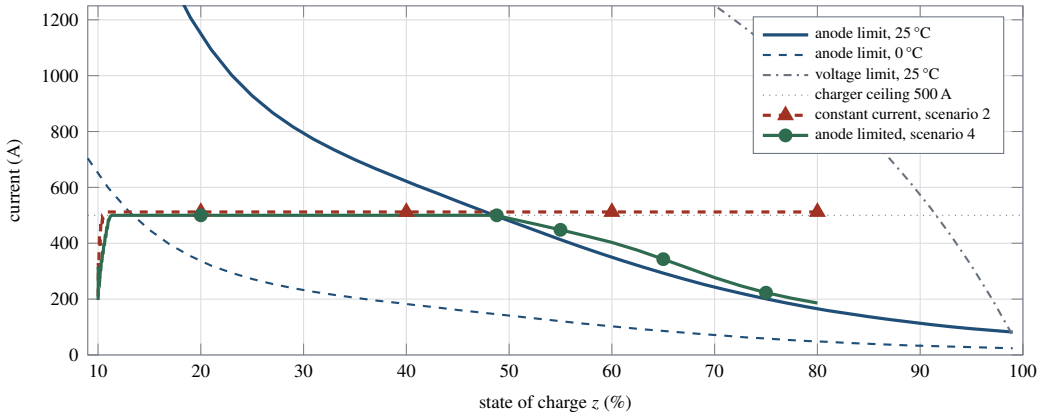


Figure 9.2 The four limits as functions of state of charge, with two measured charges drawn over them. At 25 °C the anode limit crosses the charger ceiling near 49 % and reaches 166 A at 80 %, while the voltage limit at the same temperature is still 959 A. The two isothermal curves both shift upward with the temperature a charge creates for itself. The measured traces are the current flowing at each state of charge. Both dip to 267 A in the first 0.1 min, which is the opening transient of Section 9.6.3, and are back at 500 A by 11.4 %. The constant-current trace is drawn 12 A high so that it separates from the anode-limited one, and it crosses the anode limit near 49 % and stays above it to the end. The anode limits are solid (25 °C) and dashed (0 °C), the voltage limit is dash-dotted and the charger ceiling dotted. The constant-current charge is dashed with triangles and the anode-limited charge solid with circles.

9.5 The Charge Controller

9.5.1 The Discrete Algorithm

One proportional-integral-derivative routine serves the voltage controller, the temperature controller and the coolant controller. It is the velocity-form routine of Section 1.6.2, with the derivative on the measurement and back-calculation on the integral alone. Equations (9.17) to (9.19) restate it in this chapter's symbols: γ is the action a of Chapter 1, Σ_k is the running sum S_k, u_k^u is the output before limiting v_k and u_{bias} is the bias u_b.

$$e_k = \gamma(\mathrm{SP}_k - \mathrm{PV}_k), \quad P_k = K_c e_k, \quad D_k = -K_c \tau_D \gamma \dot{\mathrm{PV}}_k \tag{9.17}$$

The direction flag γ is $+1$ when a rising measurement calls for a smaller output, which is reverse action in the ISA convention, and -1 when it calls for a larger one.

$$\begin{aligned} \Sigma_k &= \Sigma_{k-1} + (P_k - P_{k-1}) + (D_k - D_{k-1}) \\ u_k^u &= u_{bias} + \Sigma_k + I_{k-1} \\ u_k &= \mathrm{clip}\,(u_k^u,\ u_{min},\ u_{max}) \end{aligned} \tag{9.18}$$

$$I_k = I_{k-1} + \left[\frac{K_c}{\tau_I} e_k + \frac{u_k - u_k^u}{T_t} \right] \Delta t_c \tag{9.19}$$

The tracking constant T_t equals τ_I, because no loop sets one of its own. All three loops are configured with $\tau_D = 0$, so the derivative path is inactive and (9.17) reduces to a proportional term. No loop carries a rate limit on its output.

Solving (9.18) for the integral at a specified output is the tracking operation, and it serves two purposes here. It supplies the operator actuator position in manual mode, and it is the external reset applied to whichever controllers lose the selector.

Table 9.3 Constraint controllers as implemented. All five are evaluated every 0.02 min, and derivative action is off in the three that have it.

Controller	Reads	Writes	K_c	τ_I (min)	Action
charger	$\hat{V}$, P_{sp}	I	—	—	algebraic
voltage	$\hat{V}$	I	60	0.15	reverse
temperature	T_m	I	120	2.0	reverse
anode	$\hat{z}$, T_m	I	—	—	inverse map
coolant	T_m	q	14	1.5	direct

9.5.2 Four Limits and One Handle

Table 9.3 lists the four candidate controllers, the coolant loop and their default settings. The signs deserve a sentence each. More current raises the terminal voltage and raises the temperature, so the voltage and temperature controllers face a positive process gain and are reverse acting. More coolant flow lowers the temperature, so the coolant loop faces a negative gain and is direct acting.

The charger controller is algebraic rather than a loop, because the post delivers whatever the vehicle asks for up to a current ceiling and a power that is the lower of the offered power and the post rating, as shown in Equation (9.20).

$$I_P = \min\left(I_{max},\ \frac{1000\ \min(P_{sp}, P_{max})}{\max(200, \hat{V})} \right) \tag{9.20}$$

with P_{sp} and P_{max} in kilowatts and $\hat{V}$ in volts. The voltage controller acts on the pack limit $n_s V_{max}$ rather than clamping the current directly, because the terminal voltage of (9.1) includes a resistive rise that moves with temperature and age, so the current that corresponds to a given cell voltage is not a constant. The temperature controller acts on the derate setpoint T_{derate} with a gain of 120 A/°C, which is a hard pullback rather than a trim, because its job is to protect a limit and not to hold a setpoint. Both are bounded to 0 to 900 A at the controller and the selected current is then clipped to the vehicle ceiling. The charger candidate never exceeds that ceiling, so a proportional-integral winner is always below it and the second clip never acts on an integral it does not know about.

9.5.3 The Anode Limit Is a Map, Not a Loop

The fourth candidate has no measurement, so it has no error, so it cannot be a controller in the sense the other three are. What the management system carries instead is the algebraic inverse of its own model, evaluated at the signals it does have and smoothed so that its output does not step, as shown in Equation (9.21).

$$\begin{aligned} I_A^{raw} &= \mathrm{clip}\left(\frac{U_{neg}(\hat{z}) - \varphi_{SP}}{\hat{R}_{ct}(T_m, \hat{z})},\ 0,\ 900\,\mathrm{A} \right) \\ I_A^k &= \alpha_A I_A^{k-1} + (1-\alpha_A) I_A^{raw}, \qquad \alpha_A = \mathrm{e}^{-\Delta t_c/\tau_A} \end{aligned} \tag{9.21}$$

where $\hat{R}_{ct}$ is Equation (9.5) evaluated with the table error m in place of the true aging multiplier a, and τ_A defaults to 0.12 min. A production system tabulates the first line of (9.21) against state of charge and temperature and interpolates it, which is the charge current limit map, and solving the expression each scan is the same thing without the interpolation error.

Two properties of (9.21) shape everything in Section 9.6. The first is that it has no integral action and cannot be given any. Over the part of the default charge where the map owns the selector the computed potential $\hat{\varphi}$ sits between 13.9 and 14.5 mV against a 15 mV setpoint, and the residual is the filter lagging a limit that is falling rather than an offset that tuning would remove. The second is that the accuracy of the output is the accuracy of $\hat{R}_{ct}$ and of the two signals feeding it, and nothing downstream reveals an error in either. The margin φ_{SP} is therefore not a safety factor in the usual

sense. It is an explicit budget for how wrong the table is allowed to be, and Section 9.6.4 measures the exchange rate between the two.

🕮 **Pause.** Try Exercise 9.1 before reading on.

9.5.4 The Selector and Its Preload

The applied command is the smallest of the candidates that the selected architecture includes, as shown in Equation (9.22).

$$I_{cmd} = \mathrm{clip}(\min\{I_P,\ I_V,\ I_T,\ I_A\},\ 0,\ I_{max}) \tag{9.22}$$

The three selector architectures the application offers include successively more of the set. Constant current and constant voltage uses I_P and I_V, the temperature variant adds I_T, and the anode-limited architecture adds I_A. The current is driven to zero at the scan on which the counted $\hat{z}$ of (9.16) reaches the target, so $b = 1.05$ ends scenario 4 at 76.7 % true charge, and times to target below are quoted at that scan.

Each proportional-integral candidate that does not own the selector is given an external reset, so both are reset while the charger or the map holds the current. The integral is solved from (9.18) so that its output equals the applied current plus a preload Δ, capped at the loser's own proportional term $P_{j,k}$, as shown in Equation (9.23) for each loser $j \in \{V, T\}$.

$$I_j \leftarrow I_{cmd} + \min(\Delta, P_{j,k}) - u_{bias} - \Sigma_{j,k} \tag{9.23}$$

with Δ defaulting to 25 A and adjustable from 0 to 120 A. Tracking a loser to the selected current alone, with $\Delta = 0$, parks it exactly on the boundary, where the change in its own proportional term across one scan is enough to make it the winner. What follows is not an oscillation, and Section 9.6.3 reports what it is instead.

The coolant loop is independent of the selector. It acts on the thermistor reading against a coolant setpoint that defaults to 32 °C, with an output of 0 to 100 % flow, and in manual it tracks the operator slider through the same mechanism as (9.23).

9.5.5 Model Predictive Control

A fourth strategy replaces the selector by one optimization over the charging current. Every $T_s = 0.1$ min, which is five controller scans, a quadratic program plans the current over $N = 100$ steps, or 10 min, and only the first move of the plan is applied, held until the following decision, as in the predictive option of Section 1.6.3 [18, 19]. The coolant loop stays outside the plan. The controller's model has five states, the counted state of charge, the two branch voltages of (9.1), the core temperature and the thermistor reading, written from the equations of Section 9.3 with the declared values of Table 9.2 and $a = 1$, as shown in Equation (9.24).

$$\begin{aligned} \frac{\mathrm{d}z}{\mathrm{d}t} &= \frac{I}{60\,Q}, \qquad G(q) = UA_{cool}\,\tfrac{q}{100} + UA_{amb} \\ \frac{\mathrm{d}T}{\mathrm{d}t} &= \frac{60}{C_p}\left[\dot{Q}_{gen} - G(q)\,(T - T_s)\right] \\ \frac{\mathrm{d}T_m}{\mathrm{d}t} &= \frac{1}{\tau_{Tm}}\left(T - \frac{6\,I}{I_{max}} - T_m\right) \end{aligned} \tag{9.24}$$

where T_s is one heat-sink temperature that stands in for the coolant, the chiller and the cabin, q is the flow the coolant loop commands at the decision, held over the horizon, and the thermistor offset is at its design scale $s = 1$. The model is written rather than identified by step tests, which the original design called for with three states, because every gain of this plant moves with its state through the Arrhenius resistances, the z^4 kinetic term and the steep top of (9.2), while the state of charge can

move 42 points over one horizon at 500 A. It is therefore relinearized at every decision along the previous plan shifted by one step, sampled exactly with a zero-order hold, with an affine term per step that makes the linear model reproduce the nonlinear one along that plan. Fed the current actually applied in anode-limited runs of five scenarios from six starting points, the model is within 0.14 V, 0.15 °C and 0.33 mV of the logged voltage, core temperature and anode estimate one minute ahead.

The predicted outputs are the voltage of (9.1) plus a bias b_V, the core temperature T and the anode headroom $I - \hat{I}_A$, where $\hat{I}_A$ is the current at which the vehicle's own estimate would sit on its setpoint, as shown in Equation (9.25).

$$\hat{I}_A(z, T_m) = \frac{U_{neg}(z) + b_U - \varphi_{SP}}{k_r R_{ct}(T_m, z)}, \qquad k_r = \frac{\hat{R}_{ct}}{R_{ct}(T_m, \hat{z})} \tag{9.25}$$

Here $\hat{R}_{ct}$ is the believed resistance of (9.21) at the decision, R_{ct} is (9.5) at the declared values, and b_U is the difference between the equilibrium potential inside the estimate and the declared one. The anode reaches the controller only through the vehicle's estimate, so a table error m or an aged pack misleads it exactly as it misleads the map, and an edited anode parameter reaches it through that estimate in the same way. An edit of any other plant parameter never reaches its model and becomes a mismatch for the estimator. A steady-state Kalman filter on the thermistor estimates T, T_m and T_s at every scan under every strategy, with T_s a random walk that makes the temperature row offset free [20]. Its inputs are the heat of (9.12) from the measured current and the offset of the thermistor, its variances per scan are 1×10^{-4} and 9×10^{-6} °C^2 on the core and the sink against 2.5×10^{-3} °C^2 on the reading, and its gain, which depends on the flow, is computed at every 10 % of flow and interpolated. The voltage bias b_V is the filtered voltage less the model's at each decision.

The decisions are moves of the current from the value applied at the decision, scaled by $I_{ref} = 500$ A, over twelve blocks whose lengths grow from a single step for the first four to 55 steps for the last, and the plan minimizes Equation (9.26).

$$\begin{aligned} J = & -c_I \sum_{k=0}^{N-1} \frac{I_k}{I_{ref}} + S \sum_{j=1}^{12} \left(\frac{\Delta I_j}{I_{ref}} \right)^2 \\ & + \sum_{r \in \{V,T,A\}} \left(\ell_r \sigma_r + \rho_r \sigma_r^2 \right) \end{aligned} \tag{9.26}$$

where $c_I = 1$ prices the charge delivered, ΔI_j is the move of block j, $S = 1$ is the move suppression, and σ_V in volts, σ_T in degrees and σ_A in amperes are one slack each on three soft rows, $V_k \le n_s V_{max} + \sigma_V$, $T_k \le T_{derate} + \sigma_T$ on the predicted core and $I_k \le \hat{I}_{A,k} + \sigma_A$. The prices are $\ell_V = 200$, $\rho_V = \ell_T = \rho_T = 1000$, $\ell_A = 100$ and $\rho_A = 10$, and while charging every logged slack stays below 10^{-15} in all seven cases of Section 9.6.7. The charger row is hard, $0 \le I_k \le \min(I_P, I_{max}, 900\,\text{A})$ with I_P of (9.20) read as the selector reads it, and the held move is capped by I_P again at every scan. A dual active-set solver [21] handles the twelve decisions. The move suppression and the sink variance were chosen once, on scenario 12, as the largest move suppression within 1 % of the fastest charge (41.31 min) among nine settings that held every limit and moved the current no more than the selector.

A plan is rejected when the solver does not return it as optimal, when it is not finite or when it leaves the charger bounds, and the anode-limited selector then takes the current until a later plan succeeds. While the plan acts, the voltage and temperature controllers track the applied current with $\Delta = 0$ in (9.23), so a hand-over moves the current only by the winning controller's own one-scan move, 1.9 A at 15 min in scenario 12 and at most 2.9 A at twelve forced instants on six cases, after which the preload applies again. The plant runs with the parameters of the run, the instruments are those of (9.15) and (9.16), and the controller reads only the counted state of charge, the applied and measured current, the filtered voltage, the thermistor, the anode estimate and its believed resistance, the commanded flow, the charger limit and the three setpoints. In Chrome a plan took a mean of 503 to 516 µs in three runs of scenario 12, at most 10.7 ms, which is about 0.5 % of one core in real time on a desktop with 20 cores whose load average was 1.5 to 1.8.

Table 9.4 The thirteen scenarios and what each isolates.

#	Scenario	Kind	What it isolates
1	The pack at rest	Experiment	four limits at one operating point
2	Constant current, constant voltage	Demonstration	a fast charge with every gauge inside its limit
3	What that charge cost	Experiment	where in a charge the damage occurs
4	Riding the limit	Experiment	the time cost of the anode-limited taper
5	Which limit is holding the current	Experiment	selector dwell and the preload
6	A cold pack	Experiment	cold kinetics and self-heating
7	A hot afternoon	Experiment	cooling that costs time and buys life
8	The model is optimistic	Demonstration	holding the estimate and plating anyway
9	An old pack and a new pack's model	Demonstration	aging the model does not know about
10	All the way to a hundred	Experiment	the tail the anode limit creates
11	A shared charger	Experiment	relieving a constraint that is not binding
12	Four limits, one QP	Experiment	one plan against four limits
13	Challenge: ten minutes at the services	Challenge	cold, aged, optimistic and short of power

9.6 Scenarios and Measured Results

The scenario sequence of Table 9.4 meets each constraint before it meets the controller that defends it. Every number reported below comes from the application running its own deterministic model at the settings the scenario loads, with any setting a sentence names changed before the run starts, which gives the same run as carrying it through Reset. Each scenario is credited separately on its own completion rule (Section 1.6.4), when the learner performs the actions its briefing lists and the simulation reaches the stated state. The challenge is judged on the case as given, so changing a model parameter or a disturbance voids the attempt.

9.6.1 What the Old Protocol Costs

Scenario 2 is a plain constant-current charge from 10 to 80 % at 25 °C, and the first thing to record is how well it appears to go. The charger holds 500 A for all but the first 0.21 min, when the voltage controller takes the selector on five alternate scans and the command dips to 238 A (the opening transient of Section 9.6.3). The 250 kW rating never binds and the power peaks at 194 kW. The highest cell voltage reached is 4.034 V against a 4.15 V limit, so the constant-voltage phase the protocol is named for never begins. The pack peaks at 38.6 °C against a 45 °C limit. Eighty percent arrives in 16.84 min with 51.6 kWh delivered, and every instrument in the vehicle is inside its limit for the whole stop.

> **TRY IT IN THE APP** **2 · Constant Current, Constant Voltage**
>
> Load scenario 2 and press Run. Watch the dotted true line on the Anode potential strip. It crosses zero at 13.57 min and 66.4 % state of charge and reaches −61.2 mV, while the pack voltage and temperature stay inside their limits. Eighty percent arrives at 16.84 min with 3.381 Ah plated.

The anode surface crosses zero at 13.57 min and 66.4 % state of charge, reaches −61.2 mV, and stays negative to the end. 3.381 Ah of lithium deposits as metal and the pack loses 0.1035 % of its capacity on one stop. Table 9.5 puts that charge against the anode-limited one in three arrival conditions.

The room-temperature row is the commercial argument about fast charging expressed in four numbers. Riding the anode limit costs 4.50 min, which is what a driver notices, and it saves 3.381 Ah of plated lithium and a quarter of the capacity fade, which is what nobody notices. The cold row is

Table 9.5 Constant-current against anode-limited charging, 10 to 80 %, measured at the moment the target is reached.

Arrival	constant current		anode limited	
	time (min)	Q_{pl} (Ah)	time (min)	Q_{pl} (Ah)
25 °C pack, 22 °C air	16.84	3.381	21.34	0.000
38 °C pack, 42 °C air	16.84	2.204	19.66	0.000
0 °C pack, 0 °C air	16.92	13.867	44.80	0.000
capacity fade on the same charges (%)				
25 °C		0.1035		0.0779
38 °C		0.1282		0.1123
0 °C		0.1232		0.0206

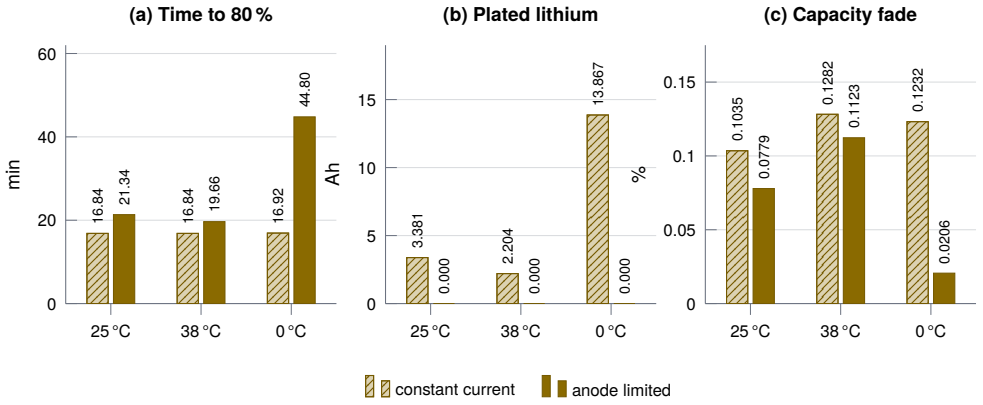


Figure 9.3 Constant-current against anode-limited charging from 10 to 80 % for the three arrivals of Table 9.5, labeled by pack temperature: (a) time to 80 %, (b) plated lithium and (c) capacity fade on the same charges. Hatched: constant current. Solid: anode limited. Notice that the constant-current charge takes nearly the same time from every arrival, while its plated lithium is largest from the cold pack, which is where the anode-limited charge pays most in time.

the one to carry away. A constant-current charge at 0 °C finishes in the usual 16.92 min and destroys 13.867 Ah of lithium inventory doing it, four times the room-temperature figure, and it looks identical on every instrument the vehicle has. The hot row runs the other way and is discussed in Section 9.6.5. Figure 9.3 draws the same table as bars.

Scenario 3 locates the damage in time by switching the map into the selector partway through the same charge, at a scripted 9 min or by hand after the scripted switch has been undone. Switching at 5, 9 or 12 min plates nothing, because scenario 2 does not cross zero until 13.57 min. Switching at 14 min costs 0.066 Ah and switching at 16 min, one minute before the end, costs 1.940 Ah, which is 57 % of the whole 3.381 Ah. The overshoot compounds because the current stays at 500 A while the true limit collapses from 524 A at 65 % to 436 at 70 and 291 A at 80 %, so nearly all the harm on a fast charge is done in its last three minutes (3.354 Ah of the 3.381 Ah, and 1.687 Ah in the final minute alone).

9.6.2 Which Constraint Is Load Bearing

Scenario 5 runs the anode-limited architecture to 95 % and reports which candidate owns the selector at every scan. The result is worth more than any tuning exercise on this plant. Of the 34.38 min

Table 9.6 Selector preload Δ swept on the scenario 4 charge to 80 %, set before the run, with a 60 min cutoff. Changes count transitions between scans.

Δ (A)	0	5	15	25	60	120
selection changes	2999	139	33	19	9	5
changes after 1 min	2950	90	1	1	1	1
held by I_V or I_T (min)	59.98	2.72	0.60	0.32	0.12	0.06
time to 80 % (min)	—	21.92	21.40	21.34	21.28	21.26
largest step after 1 min (A)	1.5	6.9	0.8	0.8	0.8	0.8
plated Q_{pl} (Ah)	0.000	0.000	0.000	0.000	0.000	0.000

charge, the charger ceiling holds the current for 9.08 min and hands over at 9.41 min and 48.8 % state of charge, the anode map holds it for 24.98 min, and the voltage and temperature controllers between them hold it for 0.32 min, all of that inside the first 0.37 min while the terminal voltage rises with the onset of current. The 250 kW power rating is never selected, and the current that would put the pack on its cell voltage limit is 1245 A at 80 % and 367 A at 95 %, both far above what the anode allows. Two of the four constraints are decorative on this pack, and the honest lesson of a four-way selector is that identifying the load-bearing constraint is worth more than tuning any of them.

Scenario 11 prices that observation. Halving the post to 120 kW between 3 and 14 min holds the current between 338 and 326 A instead of 500 A and pushes eighty percent from 21.34 to 25.32 min, a loss of 3.98 min. Firing the identical outage in scenario 4 at 14 min, in the second half of the charge, costs 0.02 min, since 21.36 against 21.34 min is the whole effect. In scenario 11 itself a second cut fired at 15 min, after the power has returned, binds only until 18.24 min and costs 0.34 min, and one fired at 18 min or later costs nothing. Relieving a constraint that is not binding is worth nothing, and a great deal of capital is spent on the wrong one.

Scenario 10 shows where the taper ends. Eighty percent arrives at 21.325 min, ninety at 29.1 min, ninety-five at 34.3 min and ninety-nine at 39.5 min on the true state of charge. The true anode limit falls from 246 to 115 A by 38.5 min and the current follows it from 185 down to 91 A. There, at 98.4 %, the voltage controller takes the current until it has tapered to $Q/20$ (10 A), where the charger ends the charge at 43.15 min and 99.75 %. The last twenty points take 21.8 min against 21.3 min for the first seventy, which is why charging networks quote ten to eighty and route planners stop there.

9.6.3 The Preload That Keeps the Selector Still

Table 9.6 sweeps the preload of (9.23) on the scenario 4 charge with everything else held.

With no preload the selection changes 2999 times in the 60 min the run is allowed, alternating between the voltage and temperature controllers at every scan, and the charge never finishes, reaching only 28.0 % by 40 min and 30.0 % by 60 min. The failure mode is not oscillation, and after the first minute the largest single-scan change in the command is only 1.5 A. Because every new winner starts from the value the previous one was tracking, the current ratchets steadily downward, from 212 A at one minute to 65 A at ten and 15 A at forty. A selector with no preload looks like a charger that is quietly giving up, which is a much harder fault to recognize on a trend than a limit cycle would be.

The remedy is cheap because the cap in (9.23) keeps the preload from standing between a controller and its own limit. Uncapped, a loser takes the current only if its proportional term moves by more than Δ in one scan (0.42 V in 1.2 s for the voltage controller), and constant current and constant voltage to a hundred percent ran 11.48 V over the pack limit, while capped it stays within 0.53 V. Twenty-five amperes costs 0.08 min on a 21.3 min charge against the largest value swept, and it reduces the selection count from 2999 to 19, with 18 of those 19 confined to the first 0.37 min. The residual activity in that window is an opening transient that no preload on the slider removes. The controller execution made when the run is initialized tracks both losers to the selected 500 A plus the preload, and in the first scan after the run starts the measured terminal voltage rises 4.8 V as the current comes on through R_0, which lowers the voltage controller’s proportional term by 288 A

Table 9.7 Kinetic table error swept at a 15 mV margin, scenario 4 conditions, 25 °C arrival.

table error m	1.00	0.90	0.80	0.70	0.60
lowest true φ (mV)	20.9	14.4	6.3	−4.1	−16.4
plated Q_{pl} (Ah)	0.000	0.000	0.000	0.187	1.628
time to 80 % (min)	21.34	20.22	19.18	18.26	17.58
fade F (%)	0.0779	0.0787	0.0797	0.0820	0.0919

at $K_c = 60\,\mathrm{A/V}$. The command dips to 238 A, which is 213 A plus the preload. The new winner's integral then climbs by about 470 A a scan against a 59 V error while the loser's proportional term falls again, and the two alternate until the voltage has settled. Raising the preload to 60 A shortens the alternation to 9 changes and 0.12 min, and 120 A to 5 changes and 0.06 min, but the first scan still dips to 273 and 333 A. The preload has to exceed the change in a losing controller's proportional term over one scan. On this plant 15 A is enough once the charge is under way, while the first scans of a charge would need more than the 120 A the slider allows. The app's design retains every constraint controller from the first scan and the shared PID tracking law. The opening dip remains a disclosed controller-startup transient rather than being hidden by temporarily gating the voltage or temperature constraints.

Pause. Try Exercise 9.2 before reading on.

9.6.4 Holding the Estimate Perfectly and Plating Anyway

Scenario 8 makes the kinetic table 30 % optimistic, which is an ordinary amount for a table fitted to a different batch three years earlier. The computed potential stays between 13.4 and 14.2 mV while the map owns the selector, so it does exactly what it was asked to do. The true anode potential reaches −12.2 mV and the pack plates 2.237 Ah. Nothing in the vehicle distinguishes this charge from a good one.

> **TRY IT IN THE APP** **8 · The Model Is Optimistic**
>
> Load scenario 8 and press Run. The kinetic table is 30 % optimistic. While the map holds the current, the computed potential stays between 13.4 and 14.2 mV. The true potential reaches −12.2 mV, and the pack plates 2.237 Ah with no warning on any instrument.

Table 9.7 converts the margin into a budget by sweeping the table error at the default 15 mV setpoint on the scenario 4 charge.

A 15 mV margin buys tolerance to a table roughly 20 % optimistic and no more. That is the sentence a design review needs, and it is a different sentence from the one a safety factor produces, because it names the model error the number is paying for. The exchange rate runs the other way as well. Under the challenge conditions, which stack a cold aged pack on a table 15 % optimistic, the suggested anode-limited configuration with a 5 mV margin plates 5.598 Ah and reaches eighty percent in 25.70 min, 15 mV plates 2.484 Ah in 27.66 min, 25 mV plates 0.024 Ah in 30.66 min and 35 mV plates nothing in 36.52 min, with the plated totals read at the 45 min judgment. Buying the last 0.024 Ah therefore costs 5.86 min, and choosing where on that curve to sit is the design decision the challenge is built around.

Scenario 9 reaches the same failure by a different road. Every resistance is 60 % higher after five years while the table is still the one calibrated when the pack was new, so the charge takes a nearly unchanged 21.38 min, runs 1.7 °C hotter and plates 3.412 Ah, which is as much as the reckless charge in scenario 2 from a strategy that plated nothing when the pack was new. Covering it with margin alone is expensive, because 30 mV brings the deposit to zero at 24.84 min, 45 mV takes 31.28 min and 60 mV takes 46.94 min. A margin that has to cover an unknown amount of aging has to cover

the worst of it on every pack all the time, which is the case for identifying the resistance on line [1] rather than widening the budget.

One result in this group is genuinely uncomfortable. The thermistor reads low while the current is high, which is an error, and it is a protective one, because the map then believes the pack is colder than it is, computes a higher kinetic resistance and allows less current. Holding the table error at 30 % and sweeping the offset scale s from 0 to 2 takes the plated lithium from 3.422 to 0.000 Ah, passing through 2.237 Ah at the scenario default of $s = 0.3$ and 0.187 Ah at the nominal $s = 1$. Fitting a better thermistor to this vehicle would make the pack worse. Two model errors of opposite sign were canceling, which is the argument for validating an inferred constraint end to end rather than instrument by instrument.

9.6.5 Cooling That Costs Time

Scenario 7 arrives at 38 °C into 42 °C air, where the chiller has lost 31 % of its capacity by (9.13). Running the coolant loop in service against holding the flow at 10 % gives 19.66 against 18.96 min to eighty percent, a peak of 40.5 against 42.7 °C, and a fade of 0.1123 against 0.1237 %. The peaks are the scorecard's, which records the hottest core temperature at any physics step since Reset. The cooled charge is the slower one, by 42 s, and that is the correct direction. A hot anode has faster kinetics by (9.5), so its plating limit is higher and the selector passes more current.

What the cooling buys is 2.2 °C of peak temperature and 9.2 % of the fade on an aging law that is Arrhenius. Judging a cooling policy on minutes gets the sign of the answer wrong, and the scorecard reports peak temperature and fade beside the time for that reason. The same asymmetry runs through the whole application. Speed is visible today and the price is paid in three years, and the controller is where somebody has to decide between them on the driver's behalf.

🕮 **Pause.** Try Exercise 9.3 before reading on.

9.6.6 The Cold Arrival and the Graded Challenge

Scenario 6 arrives at 0 °C. The anode-limited charge takes 44.80 min against 21.34 min from a warm pack, which makes the arrival temperature the single largest influence on the length of the stop. The current climbs from 216 A at half a minute to a peak of 414 A at 1.5 min and then falls, to 372 A at two minutes, 303 A at five and 261 A at ten. The climb is not the pack warming itself. Until 1.56 min the selector changes hands 76 times, almost all of them between the voltage and temperature controllers as in the opening transient of Section 9.6.3, and the climb is their recovery from the opening dip. The true plating limit and the map both fall from the first scan, because the equilibrium potential of (9.4) drops from 266 to 139 mV between 10 and 20 % state of charge faster than self-heating lowers R_{ct}, and the pack has reached only 11.0 °C by ten minutes. With the arrival temperature set to 15 °C and the run restarted with Reset, the same charge in the same 0 °C air takes 27.40 min. This is the quantitative case for preconditioning, because heat put in from the drivetrain on the way to the charger is cheaper than heat bought in charging time.

> ✦ **DID YOU KNOW? A Cold Pack Looks Exactly Like a Warm One**
>
> From the simulator: at a 0 °C arrival the constant-current charge reaches eighty percent in 16.92 min and plates 13.867 Ah, four times the room-temperature figure, while the anode-limited charge plates nothing and takes 44.80 min (Table 9.5).

The graded challenge stacks the failures. The pack arrives at 5 °C into 6 °C air, aged 30 %, on a table 15 % optimistic, with the post halving between 6 and 16 min, and it opens in the constant-current architecture with a 5 mV margin, the detuned settings, zero preload and a fixed 20 % coolant flow. As loaded it reaches eighty percent in 21.64 min and has plated 14.196 Ah by the 45 min judgment, 284 times the limit, and it projects a 62.6 % loss, although it peaks at only 28.0 °C. The target is eighty percent with less than 0.05 Ah plated, a peak under 45 °C and a projected loss under 20 % over five

Table 9.8 Anode-Limited Selector Against the Predictive Controller

Case	Structure	Time to target (min)	Hottest core °C (min)	Core over T_{derate} (min)	Largest $V - n_s V_{max}$ V (min)	Over by 0.1 V (min)	Lowest $\hat{\varphi} - \varphi_{SP}$ (mV)	Plated (Ah)	Current travel (A)
4	selector	21.345	37.40 (12.53)	0.00	−17.45 (21.32)	0.00	−1.14	0.000	796
	predictive	21.525	37.35 (12.53)	0.00	−17.49 (21.49)	0.00	−0.11	0.000	802
6	selector	44.805	15.70 (26.81)	0.00	−17.64 (44.80)	0.00	−8.04	0.000	1728
	predictive	44.585	15.94 (26.42)	0.00	−17.68 (44.56)	0.00	−0.06	0.000	872
7	selector	19.665	40.53 (12.39)	6.58	−17.40 (19.64)	0.00	−1.28	0.000	650
	predictive	20.405	40.03 (10.36)	3.82	−17.47 (20.37)	0.00	−0.11	0.000	835
9	selector	21.385	39.11 (9.84)	0.00	−14.21 (21.35)	0.00	−1.40	3.412	1015
	predictive	21.445	39.11 (9.56)	0.00	−14.30 (21.42)	0.00	−0.13	2.997	802
10	selector	43.145	37.40 (12.53)	0.00	0.10 (38.92)	0.00	−1.14	0.000	796
	predictive	43.605	37.35 (12.53)	0.00	0.01 (39.20)	0.00	−0.11	0.000	802
12	selector	38.405	38.71 (12.39)	12.81	0.09 (34.44)	0.00	−1.22	0.000	1072
	predictive	41.625	35.95 (6.37)	0.00	0.01 (37.10)	0.00	−0.10	0.000	957
13	selector	30.665	26.52 (23.97)	0.00	−15.84 (30.66)	0.00	−5.88	0.024	2103
	predictive	30.065	26.90 (23.24)	0.00	−15.91 (30.03)	0.00	0.01	0.002	955

Cases are the scenarios of Table 9.4 (4 riding the limit, 6 a cold pack, 7 a hot afternoon, 9 an old pack, 10 to a hundred, 12 four limits, one QP, and 13 the challenge at its suggested settings). The selector is the anode-limited selector. The derate setpoint T_{derate} is 36 °C in scenario 12 and 40 °C elsewhere. Time to target is the scorecard's, latched when the vehicle's count reaches the target or, in scenario 10, when the current has tapered to $Q/20$ on the voltage limit. The hottest core with its time, the minutes over T_{derate}, the largest voltage excess with its time, the minutes more than 0.1 V over and the lowest estimate margin are taken while charging, before the target is reached. Current travel is the scorecard's total movement of the charging current over the whole run.

hundred charges, and the answer is mostly structural. The map has to be in the selector, the margin has to be widened to 25 mV or beyond, and the coolant loop has to be put back on temperature, which on a pack this cold holds the flow at zero and keeps the heat in the cells. With the suggested settings (anode limited, 25 mV, the tuned gains and preload, the coolant loop on temperature) the charge takes 30.66 min, plates 0.024 Ah, peaks at 26.5 °C and projects an 18.9 % loss. It passes with 0.026 Ah and 1.1 percentage points to spare, and revealing the suggestion before the run and carrying it through Reset give the same run. Two tuning values matter as well. With the structure and the margin changed but the 1.4 min map filter and the zero preload kept, the charge stands at 79.05 % at 45 min with 0.186 Ah plated, while restoring those two passes even with the detuned proportional-integral gains, in 29.78 min with 0.021 Ah. The suggested settings with the shipped 20 % coolant flow plate 0.169 Ah and fail. What remains after that cannot be tuned away, because a cold pack is slow and the first five minutes are spent whatever anybody does.

9.6.7 Comparison With the Predictive Controller

Table 9.8 sets the anode-limited selector against the predictive controller of Section 9.5.5 on seven cases, each run for 60 min (the challenge for 45 min at its suggested settings) with the same events, instruments and coolant loop, and with the predictive settings of scenario 12 on every case. Neither receives a preview, which the application does not have, and the predictive controller solved 600 plans per hour with none rejected.

Scenario 12 was built so that every limit holds the predictive controller's current for a stretch. The pack arrives at 30 °C in 38 °C air with a 95 % target, a cell limit of 4.08 V (391.7 V for the pack), a derate setpoint of 36 °C and the post cut to 120 kW from 4 to 9 min. Under the predictive controller the charger holds the current from 0.32 to 5.81 min, the core temperature to 19.01, the anode estimate to 37.03 and the voltage to the end, and the target arrives at 41.625 min. The selector arrives at 38.405 min, but its core reaches 38.71 °C at 12.39 min and spends 12.81 min above 36 °C while its thermistor stays at least 2.58 °C below it, as shown in Figure 9.4. Its voltage controller holds the pack from 33.98 min, at most 0.09 V over the limit. The predictive controller holds its core at 35.85 °C with 320 A flowing at 12.4 min and rides the voltage limit only from 37.03 min, exceeding it by 0.01 V at most.

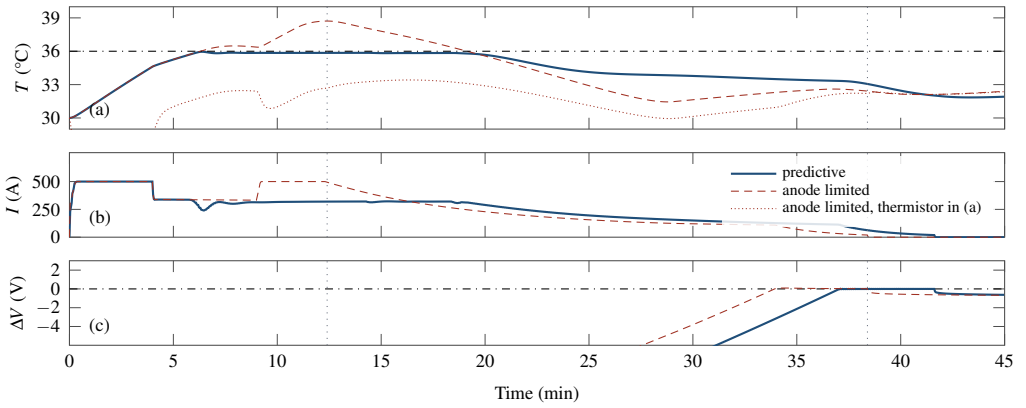


Figure 9.4 Scenario 12 under the predictive controller and under the anode-limited selector, from the same arrival and the same post cut from 4 to 9 min. The predictive controller is solid, the anode-limited selector densely dashed, its thermistor densely dotted, and the setpoint and zero lines dash-dotted. The vertical dotted lines mark 12.4 min, where the selector's core is at 38.7 °C and the predictive controller holds 35.9 °C, and 38.4 min, where the selector reaches 95 %. (a) Core temperature, the selector's thermistor and the 36 °C derate setpoint. (b) Current flowing. (c) Pack voltage less its limit, $\Delta V = V - n_s V_{max}$.

The selector passes the temperature limit because its temperature controller reads the thermistor, which sits below the core by the offset of (9.15). Relaxing the predictive controller's core row with a derate setpoint of 55 °C brings it to 38.79 min, so 0.38 min of its 3.22 min remains once it is allowed what the selector took.

The hot afternoon of scenario 7 is a different kind of loss. There the selector holds every limit on the instrument it reads, with its thermistor at least 2.00 °C under the 40 °C setpoint and its voltage 17.40 V under its limit, while its core, which no controller reads, reaches 40.53 °C at 12.39 min and spends 6.58 min of the charge above 40 °C. The predictive controller applies the setpoint to its estimate of the core instead, its core exceeds the setpoint by at most 0.03 °C, and it is 0.74 min slower. With that row relaxed it takes 19.81 min, so 0.60 min of the difference is the stricter reading of the setpoint and 0.14 min the remainder. Its peak temperature on the scorecard, 40.24 °C, is set at 60 min, after the charge, as the idle pack warms toward the 42 °C air with the chiller off. On the plain charge of scenario 4 neither structure reaches its voltage or temperature limit and the predictive controller is 0.18 min slower, of which 0.10 min is the move price, since a move suppression of 0.1 gives 21.425 min. From the cold arrival it is 0.22 min faster with half the current travel, and on the aged pack both plate (2.997 against 3.412 Ah) because both read the same new-pack estimate.

Charging to a hundred percent brings the two together. Both hold the voltage limit from 38.5 min (0.10 V and 0.01 V over at most), and since the open-circuit voltage of a full cell is the 4.15 V limit itself, both end at $Q/20$, at 43.145 min and 43.605 min. With the challenge's suggested settings the predictive controller reaches eighty percent at 30.065 min against 30.665 min and plates 0.002 Ah against 0.024 Ah. The predictive controller is therefore not a faster charger on this pack. In scenario 12 most of its extra time is a limit the selector does not keep on the quantity it protects, while on the hot afternoon the minutes are its stricter reading of the derate setpoint and on the plain charge they are its price on moves. Figure 9.5 shows the application during the anode-limited charge of scenario 4.

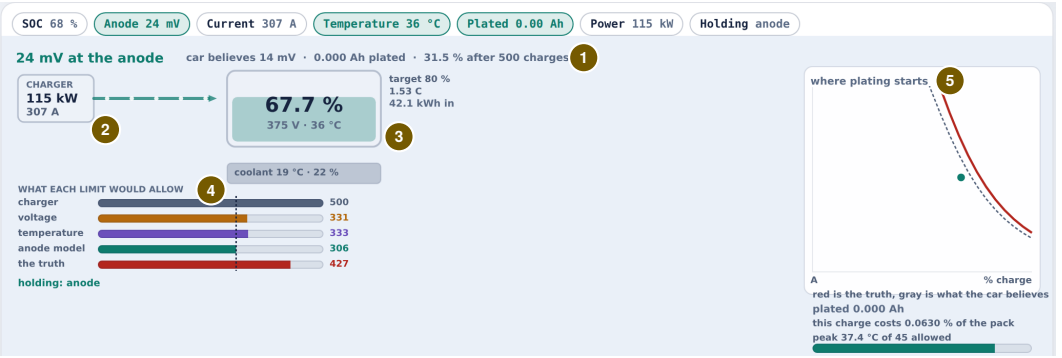


Figure 9.5 Anode-limited charging in scenario 4 at 15 min, some way past the handover from the charger ceiling, cropped to the plant scene. (1) The anode line: the true potential is 24.0 mV while the computed one is 13.9 mV, and nothing has plated. (2) The charger, with 307 A flowing. (3) The pack at 67.7 % state of charge, with the coolant loop beneath it. (4) The four candidate currents on one axis, 500 A from the charger, 331 on voltage, 333 on temperature and 306 from the anode model, with the true anode limit of 427 A drawn beside them and the anode named as the one holding. (5) The plating map with its believed and true curves, and beneath it the plated total of 0.000 A h.

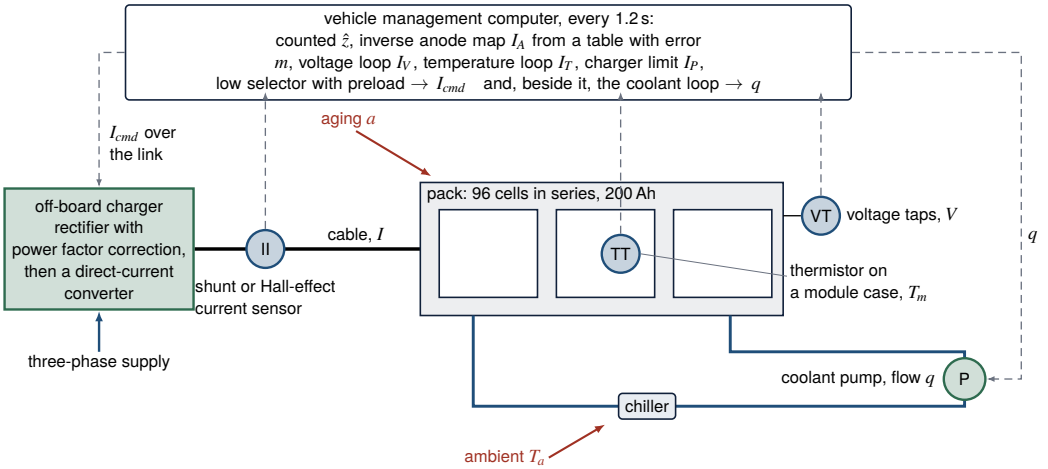


Figure 9.6 The chapter's loops drawn with their hardware. The current sensor II on the cable, the voltage taps VT and one thermistor TT on a module case are all the management computer reads. Every 1.2 s it computes four candidate currents, sends the lowest to the off-board charger over the communication link, and sets the coolant pump. Ambient temperature T_a acts on the chiller and cell aging a on the pack, and the table error m sits inside the computer. Notice that no device reads the anode surface potential, the quantity that ends the charge.

9.7 Technology in Practice

The instruments and the post of Section 9.3 are, in a vehicle, a current sensor, voltage taps, thermistors, a management computer, a coolant pump and an off-board charger. Figure 9.6 draws the chapter's loops with that hardware in place of the schematic's symbols.

What Measures It

The quantity that ends a fast charge has no field instrument. Plating can occur when the local potential of the negative electrode is below zero against lithium [15], and no vehicle in service carries a reference electrode that reports it (Section 9.1). What the management system does read is the pack current, the terminal voltage and a few temperatures. A current can be measured as the voltage across a precision shunt resistor of small value, or without breaking the circuit by a Hall-effect sensor that clamps around the conductor [22]. Whichever is fitted, the counted state of charge integrates its error, which is the bias b of Equation (9.16).

> **TECHNOLOGY** **Sensor: Thermistors on the Modules**
>
> A thermistor is a piece of metal oxide whose resistance changes with temperature. It is highly sensitive and nonlinear, and it is typically used where high accuracy is unimportant [22]. The current that reads its resistance also heats it, which adds a positive error [22]. A national laboratory study of fast charging noted that if temperature and voltage sensors could be placed on every cell, the weaker and hotter cells could be identified [15]. The chapter's thermistor sits on the module case, reads low in proportion to the current and is filtered with a 0.25 min time constant.

What Moves It

Two final elements act on the pack. The charger sets the current, and a pump sets the coolant flow. Liquid cooling, typically a mixture of ethylene glycol and water, is the preferred thermal management for most battery vehicles. Its many connections raise the potential for failure, and a failed system could let the liquid short out adjacent cells [17]. The chapter's coolant controller writes the flow q of Table 9.3, and its chiller of Equation (9.13) stands in for the refrigeration that removes the heat.

> **TECHNOLOGY** **Final Element: The Off-Board Direct-Current Charger**
>
> A direct-current fast charger converts three-phase alternating voltage in two power stages. A rectifier with power factor correction makes an intermediate direct voltage, and a second converter regulates the direct voltage the battery needs. Galvanic isolation comes from a line-frequency transformer ahead of the rectifier or from a high-frequency transformer inside the second stage, and identical modules run in parallel when one is not enough [23]. The vehicle's charge controller tells the off-board charger the battery's constraints, and the two coordinate the charging voltage and current [16]. The chapter's post follows the vehicle's command with a 0.02 min time constant up to a 500 A ceiling.

Where the Controller Runs

The selector of Section 9.5 runs in the vehicle's management computer, an embedded controller of the kind that replaced analog mechanical controls in machines and engines [24]. The vehicle and the off-board charger coordinate the charging voltage and current over a communication link [16]. Control loops of this kind run with cycle times from milliseconds to minutes [24]. In the chapter the management system executes every 0.02 min, which is 1.2 s, on a physics step of 0.3 s, and the predictive controller decides every 0.1 min. The inverse map, the voltage and temperature loops and the low selector with its preload are one block of that software, and the coolant loop runs beside it.

> **IN PRACTICE** **The Standards Between Vehicle and Post**
>
> Conductive charging in North America is defined in SAE J1772, and IEC 62196-3 defines four vehicle coupler configurations for direct-current fast charging [23]. IEC 61851-23 covers the direct-current charging station and requires that each output circuit be isolated from the others, and IEC 61851-24 covers the digital communication between station and vehicle for control of the charge [23]. Cable weight is a practical limit. A 50 kW cable weighs about 9 kg, and at 400 V a cable for 200 kW can exceed the 22.7 kg a single person may safely lift [23].

What Is Modernizing It

Four developments touch this loop. The first is voltage. A study in 2017 took 800 to 1000 V packs and more than 400 kW of charging power as the design point for future vehicles, and a higher charging voltage reduces the size of the cable between charger and vehicle [16]. The second is the cable. Liquid cooling of the cable reduces its thermal stress and makes a smaller and lighter cable feasible [23]. The third is the station. A station can share one central rectifier on a direct-current bus, or use a solid-state transformer that rectifies, steps down and isolates in one unit [23]. The fourth is communication. The vehicle must send its battery constraints to the off-board charger, and a 1000 V, 400 kW link could give an attacker an enticing target [16]. None of the four measures the anode, and the open challenges below concern that gap.

9.8 Limitations

Nothing in this application supports a claim about a real cell. The anode criterion is lumped, the plating law has no nucleation threshold and no morphology, the pack has no cell-to-cell spread, and the aging law has two terms where a life prediction needs many. The projections over five hundred charges are the arithmetic of Equation (9.8) repeated, and the comparisons between strategies are the result while the absolute ampere hours and percentages are not. Section 9.3.8 states where each simplification stops holding.

The scope is narrower than the domain in three further respects. The state estimator behind the selector is plain coulomb counting and a table lookup, with no Kalman filter, no on-line resistance identification and no adaptation, which is deliberate because the subject of the application is what happens when a model does not adapt [8]. Only charging is modeled, so regenerative braking, driving loads and the discharge side of the aging problem are absent. The vehicle and post negotiate nothing, since the post is Equation (9.14) and a slider.

Two properties of the numerics are convenient and unrealistic. A frozen integration step and a frozen scan period reproduce the same trajectory on any computer, while a real pack controller has jitter, quantized measurements and a scan order that moves. The absence of any noise term means the selector never has to arbitrate between two candidates whose measurements are rattling, which is precisely the condition under which the preload of (9.23) earns most of its keep in a plant, and the deterministic chatter reported in Section 9.6.3 understates it. Measurement noise on a loser near its limit would also make the cap of (9.23) rattle, which the deterministic model does not exercise.

The predictive controller's model leaves out the coolant node, the chiller and the cabin, which it lumps into one sink temperature, and it holds the coolant flow over the horizon, so its prediction of the core ten minutes ahead runs up to 5.9 °C hot where the coolant loop opens later in the window. That prediction is not displayed. Its visible consequence is a predicted state of charge that reads low, by 3.8 points on average against the charge reached ten minutes later in scenario 12. The model also omits capacity fade, the true aging and the true kinetic resistance, so it inherits the error of the vehicle's estimate in full.

OPEN CHALLENGE Detecting Plating on Board

Plating can occur when the local potential of the negative electrode falls below zero against lithium, and it grows with current density and as the temperature falls [15]. Methods that detect it without taking the cell apart exist in the literature: high-precision coulometry, small changes in cell volume, calorimetry, and a voltage plateau while the plated metal strips back [15]. None of them is an instrument a vehicle carries on every charge, and the 2017 assessment listed methods to detect and prevent plating as a research need, since plating is a safety and performance issue [15]. Progress would be a signal in service that tells a computed margin from a real one.

9.9 Discussion

The result that generalizes past batteries is the one about the preload, and it generalizes because it does not depend on the physics. Any low selector whose losing controllers are tracked exactly to the selected output has candidates sitting on the boundary, and any change in a proportional term across one scan is then enough to hand the selection over. Whether the outcome is a downward ratchet or a limit cycle depends on whether the new winner inherits the old winner's value, and with external reset it does, so the failure is a slow drift of the manipulated variable toward one end of its range. A drift is far harder to see on a trend than a cycle, and the plant looks starved rather than unstable. The limiter selector of a jet engine in Volume 4, Chapter 3, whose every integrator tracks the fuel commanded, has the same structure. The remedy is a preload larger than the per-scan movement of the fastest losing controller, which Table 9.6 puts between 5 and 15 A on this plant once a charge is under way. The opening scans are the exception, because the ohmic step moves the voltage controller by 288 A in one scan, and a selector that must be quiet from the first scan needs the step itself removed, by ramping the command or by holding the losers tracked for the first few scans.

The result that matters most inside the domain is the one about margin. An inferred constraint is defended by a number chosen in advance, and that number is paying for model error rather than for uncertainty in the plant. The distinction has consequences for how the number is justified, because a tolerance to a 20 % optimistic table is an auditable statement about a validation program while a safety factor is not. The sticky-margin override of the spray dryer in Volume 5, Chapter 10 defends another constraint that is inferred rather than measured. It also sets the economics of adaptation. On the aged pack of scenario 9 a 30 mV margin plates nothing and adds 3.50 min to the 21.34 min a new pack takes, while a margin chosen to cover an unknown amount of aging has to be wider still and 45 mV adds 9.94 min. Identifying the resistance from the voltage response would recover most of that [1], which is the trade a fleet operator would price.

OPEN CHALLENGE A Safe Envelope for Uneven Aging

Cells in one pack age at slightly different rates, so after a fast charge some sit at a higher state of charge than others, and the management system has to limit the current through the weaker cells to prevent overheating [15]. The 2017 assessment asked for a management system sensitive enough to compensate for non-uniform aging, and for research to identify a safe envelope beyond which major performance and safety concerns arise [15]. Progress would be limits that follow each pack's aging rather than a table fitted when it was new.

The plant is also a reasonable target for the dynamic optimization and estimation methods of other volumes in this series. Equations (9.1) to (9.8) with the plating rate as a soft constraint and the charge time as the objective is a small nonlinear program of the kind a dynamic optimization package handles [25], and posing it that way replaces the selector and the margin with one explicit constraint and one explicit horizon [13]. The estimation problem sits alongside it, since the same equations with the terminal voltage as the measurement and R_{ct} as an estimated parameter are a moving horizon estimator, and running the two together is the adaptive scheme the aged pack argues for.

9.10 Conclusion

A vehicle pack on a fast charger serves in this chapter as an interactive laboratory for constraint control in which the binding constraint has no instrument. Nine states carry the state of charge, two polarization voltages, the pack and coolant temperatures, the charger current and three counters, and four candidate controllers write to one current through a low selector. Three of the four are proportional-integral loops closed on a measured error. The fourth is the algebraic inverse of a kinetic model, filtered and looked up, and it holds its computed potential between 13.9 and 14.5 mV against a 15 mV setpoint whether or not the pack is anywhere near that value. On this pack the constant-current protocol reaches 80 % in 16.84 min and deposits 3.381 Ah of metallic lithium for 0.1035 % of capacity, while the anode-limited strategy takes 21.34 min, deposits nothing and fades 0.0779 %. A table 30 % optimistic still plates 2.237 Ah with the estimate held perfectly, and a 15 mV margin covers a table roughly 20 % optimistic and no more. Removing the selector preload changes the selection 2999 times in 60 min and ratchets the current from 212 to 15 A without finishing the charge. The optional predictive controller holds the four limits in one plan, and in scenario 12 it keeps the core at 35.95 °C and the voltage within 0.01 V of its limit for a charge 3.22 min longer than the selector’s. Two of the four constraints are never selected on a charge to eighty percent for more than 0.32 min, which is the general observation the application is built to deliver, since knowing which constraint carries the plant is worth more than tuning the ones that do not.

KEY POINTS

- No instrument in the vehicle reads the potential at the graphite surface, the limit that ends a fast charge.
- From 25 °C, constant current reaches 80 % in 16.84 min and plates 3.381 Ah, and the anode-limited charge takes 21.34 min and plates nothing.
- A 15 mV margin covers a table roughly 20 % optimistic and no more.
- Without a preload the selection changes 2999 times in 60 min and the charge never finishes.
- Knowing which constraint carries the plant is worth more than tuning the ones that do not.

Where else this applies. A low selector over limiters that guard a margin no sensor reads also sets the fuel of the turbofan in Volume 4, Chapter 3, and an unmeasured core temperature is controlled in Volume 5, Chapter 11.

References

[1] F. F. Oehler, X. Deuschl, K. Nürnberger, A. Graule, S. Kücher, T. Roth, A. Adam, J. Li, R. Mörtel, and A. Jossen, “Online adaptive anode potential-controlled fast charging of lithium-ion cells using a validated electrochemical model-based virtual reference electrode,” *Journal of Power Sources*, vol. 608, p. 234620, 2024.

[2] P. Arora, M. Doyle, and R. E. White, “Mathematical modeling of the lithium deposition overcharge reaction in lithium-ion batteries using carbon-based negative electrodes,” *Journal of The Electrochemical Society*, vol. 146, no. 10, pp. 3543–3553, 1999.

[3] T. Waldmann, B.-I. Hogg, and M. Wohlfahrt-Mehrens, “Li plating as unwanted side reaction in commercial Li-ion cells – a review,” *Journal of Power Sources*, vol. 384, pp. 107–124, 2018.

[4] T. Ohzuku, Y. Iwakoshi, and K. Sawai, “Formation of lithium-graphite intercalation compounds in nonaqueous electrolytes and their application as a negative electrode for a lithium ion (shuttlecock) cell,” *Journal of The Electrochemical Society*, vol. 140, no. 9, pp. 2490–2498, 1993.

[5] Y. Ji, Y. Zhang, and C.-Y. Wang, “Li-ion cell operation at low temperatures,” *Journal of The Electrochemical Society*, vol. 160, no. 4, pp. A636–A649, 2013.

[6] F. G. Shinskey and J. P. Shunta, “Selective, override, and limit controls,” in *Process Control*. Elsevier, 1995, pp. 112–118.

[7] R. Hanus, M. Kinnaert, and J.-L. Henrotte, “Conditioning technique, a general anti-windup and bumpless transfer method,” *Automatica*, vol. 23, no. 6, pp. 729–739, 1987.

[8] N. A. Chaturvedi, R. Klein, J. Christensen, J. Ahmed, and A. Kojic, “Modeling, estimation, and control challenges for lithium-ion batteries,” in *Proceedings of the 2010 American Control Conference*, 2010, pp. 1997–2002.

[9] S. S. Zhang, “The effect of the charging protocol on the cycle life of a Li-ion battery,” *Journal of Power Sources*, vol. 161, no. 2, pp. 1385–1391, 2006.

[10] P. H. L. Notten, J. H. G. Op het Veld, and J. R. G. van Beek, “Boostcharging Li-ion batteries: A challenging new charging concept,” *Journal of Power Sources*, vol. 145, no. 1, pp. 89–94, 2005.

[11] M. Doyle, T. F. Fuller, and J. Newman, “Modeling of galvanostatic charge and discharge of the lithium/polymer/insertion cell,” *Journal of The Electrochemical Society*, vol. 140, no. 6, pp. 1526–1533, 1993.

[12] R. Klein, N. A. Chaturvedi, J. Christensen, J. Ahmed, R. Findeisen, and A. Kojic, “Optimal charging strategies in lithium-ion battery,” in *Proceedings of the 2011 American Control Conference*, 2011, pp. 382–387.

[13] H. E. Perez, X. Hu, S. Dey, and S. J. Moura, “Optimal charging of Li-ion batteries with coupled electro-thermal-aging dynamics,” *IEEE Transactions on Vehicular Technology*, vol. 66, no. 9, pp. 7761–7770, 2017.

[14] A. Tomaszewska, Z. Chu, X. Feng, S. O’Kane, X. Liu, J. Chen, C. Ji, E. Endler, R. Li, L. Liu, Y. Li, S. Zheng, S. Vetterlein, M. Gao, J. Du, M. Parkes, M. Ouyang, M. Marinescu, G. Offer, and B. Wu, “Lithium-ion battery fast charging: A review,” *eTransportation*, vol. 1, p. 100011, 2019.

[15] S. Ahmed, I. Bloom, A. N. Jansen, T. Tanim, E. J. Dufek, A. Pesaran, A. Burnham, R. B. Carlson, F. Dias, K. Hardy, M. Keyser, C. Kreuzer, A. Markel, A. Meintz, C. Michelbacher, M. Mohanpurkar, P. A. Nelson, D. C. Robertson, D. Scoffield, M. Shirk, T. Stephens, R. Vijayagopal, and J. Zhang, “Enabling fast charging – a battery technology gap assessment,” *Journal of Power Sources*, vol. 367, pp. 250–262, 2017.

[16] A. Meintz, J. Zhang, R. Vijayagopal, C. Kreutzer, S. Ahmed, I. Bloom, A. Burnham, R. B. Carlson, F. Dias, E. J. Dufek, J. Francfort, K. Hardy, A. N. Jansen, M. Keyser, A. Markel, C. Michelbacher, M. Mohanpurkar, A. Pesaran, D. Scoffield, M. Shirk, T. Stephens, and T. Tanim, “Enabling fast charging – vehicle considerations,” *Journal of Power Sources*, vol. 367, pp. 216–227, 2017.

[17] M. Keyser, A. Pesaran, Q. Li, S. Santhanagopalan, K. Smith, E. Wood, S. Ahmed, I. Bloom, E. Dufek, M. Shirk, A. Meintz, C. Kreuzer, C. Michelbacher, A. Burnham, T. Stephens, J. Francfort, B. Carlson, J. Zhang, R. Vijayagopal, K. Hardy, F. Dias, M. Mohanpurkar, D. Scoffield, A. N. Jansen, T. Tanim, and A. Markel, “Enabling fast charging – battery thermal considerations,” *Journal of Power Sources*, vol. 367, pp. 228–236, 2017.

[18] S. J. Qin and T. A. Badgwell, “A survey of industrial model predictive control technology,” *Control Engineering Practice*, vol. 11, no. 7, pp. 733–764, 2003.

[19] D. Q. Mayne, J. B. Rawlings, C. V. Rao, and P. O. M. Scokaert, “Constrained model predictive control: Stability and optimality,” *Automatica*, vol. 36, no. 6, pp. 789–814, 2000.

[20] G. Pannocchia and J. B. Rawlings, “Disturbance models for offset-free model-predictive control,” *AIChE Journal*, vol. 49, no. 2, pp. 426–437, 2003.

[21] D. Goldfarb and A. Idnani, “A numerically stable dual method for solving strictly convex quadratic programs,” *Mathematical Programming*, vol. 27, no. 1, pp. 1–33, 1983.

[22] T. R. Kuphaldt, *Lessons in Industrial Instrumentation*, version 2.33 ed. Open textbook, Creative Commons Attribution 4.0 license, ibiblio.org/kuphaldt/socratic/sinst, 2024.

[23] H. Tu, H. Feng, S. Srdic, and S. Lukic, “Extreme fast charging of electric vehicles: A technology overview,” *IEEE Transactions on Transportation Electrification*, vol. 5, no. 4, pp. 861–878, 2019.

[24] K. Stouffer, M. Pease, C. Tang, T. Zimmerman, V. Pillitteri, S. Lightman, A. Hahn, S. Saravia, A. Sherule, and M. Thompson, “Guide to operational technology (OT) security,” National Institute of Standards and Technology, Gaithersburg, MD, Special Publication 800-82r3, 2023.

[25] L. D. R. Beal, D. C. Hill, R. A. Martin, and J. D. Hedengren, “GEKKO optimization suite,” *Processes*, vol. 6, no. 8, p. 106, 2018.

9.11 Exercises

9.1 Concept check · 2 min

While the anode map holds the current in scenario 4, the computed anode potential sits between 13.9 and 14.5 mV against its 15 mV setpoint. A colleague proposes adding integral action to the anode candidate to remove the offset. Which assessment is right?

(a) It would remove the offset and protect the pack better, since the true potential would then sit on the setpoint

(b) It would remove the offset but wind up while the map loses, so it needs the same preload as the other two loops

(c) It would not help, since the offset comes from the thermistor reading low and a better thermistor removes it

(d) It cannot be done in a useful sense, since nothing measures the potential and the residual is the filter lagging a falling limit

9.2 Concept check · 1 min

Scenario 5 is run with the Selector preload set to 0 A before Run. What does the charge do?

(a) The selection changes at almost every scan and the current ratchets steadily down, so the charge never finishes

(b) The voltage and temperature controllers enter a growing limit cycle, and the charger trips on the current swings

(c) The charger keeps the selector for the whole charge, and the voltage limit ends the charge early

(d) Nothing changes after the first minute, because the preload matters only in the opening transient

9.3 Concept check · 2 min

Scenario 7 arrives at 38 °C into 42 °C air. The anode-limited charge is run once with the coolant loop on temperature and once with the flow fixed at 10 %. Which statement is right?

(a) The cooled charge is faster, because a cooler pack has a lower ohmic resistance and a smaller voltage rise

(b) The cooled charge is slower, because a cooler anode has slower kinetics and a lower plating limit

(c) The two take the same time, because the anode limit depends on the state of charge and not on temperature

(d) The uncooled charge is slower, because the temperature controller cuts the current back as the pack heats

9.4 Theory and calculation · 6 min

The default cell has $U_0 = 0.085\,\mathrm{V}$, $U_A = 0.60\,\mathrm{V}$, $k_U = 12$, $R_{ct}^{0} = 1.2 \times 10^{-4}\,\Omega$ and $k_R = 8.0$, with no aging ($a = 1$). Work at 25 °C, where the Arrhenius factor of Equation (9.5) is one.

(a) Find U_{neg} and R_{ct} at 50 % and at 80 % state of charge. *Checkpoint:* 86.5 mV and 0.180 mΩ, then 85.0 mV and 0.513 mΩ.

(b) Find the plating current I_{lim} at both states of charge, and say which limit binds at 50 % on a 500 A charger. *Checkpoint:* 480 A and 166 A, so the charger binds.

(c) Find the current the map allows with $\varphi_{SP} = 15\,\mathrm{mV}$ when its signals and its table are exact. *Checkpoint:* 397 A and 137 A.

9.5 Theory and calculation · 7 min

Use Table 9.2. Absolute temperature is $T + 273.15\,\mathrm{K}$ and $T_{ref} = 298.15\,\mathrm{K}$.

(a) Find the factor by which the kinetic resistance at 0 °C exceeds its value at 25 °C, and the plating current at half charge from a 0 °C pack. *Checkpoint:* 3.41 and 141 A.

(b) Find the same factor for the ohmic resistance, which has $E_R = 3600\,\mathrm{K}$. *Checkpoint:* 3.02.

(c) Find the heat 500 A deposits in the nominal R_0^0 at 25 °C, and the chiller capacity at 42 °C ambient from Equation (9.13). *Checkpoint:* 5.88 kW against 4.51 kW, a loss of 31 %.

9.6 Theory and calculation · 8 min

The map holds its estimate on φ_{SP}, using $\hat{R}_{ct} = m R_{ct}$ in place of the true R_{ct}. Take the counted state of charge and the temperature it reads as exact.

(a) Show that the true potential is then $\varphi = U_{neg} - (U_{neg} - \varphi_{SP})/m$. *Checkpoint:* The map's current is $(U_{neg} - \varphi_{SP})/(mR_{ct})$.

(b) On the plateau, $U_{neg} = 85.4\,\text{mV}$. Find the smallest m a 15 mV margin tolerates, and the true potential at $m = 0.70$. *Checkpoint:* $m = 0.824$, then $-15.2\,\text{mV}$.

(c) Find the margin that keeps $\varphi \geq 0$ at $m = 0.70$, and at the challenge's believed-to-true ratio $0.85/1.3$. *Checkpoint:* 25.6 mV, then 0.654 and 29.6 mV.

9.7 App challenge · 8 min

Use the default seed and the speed 5 (25 min takes 5 s of wall time). Run each case to 25 min and read the scorecard tiles Time to target, Plated, Fade this charge and After 500 charges. The model has no noise, so the tiles should match the answers in their last digit.

(a) Load scenario 2, Constant current, constant voltage, and run it as shipped. *Checkpoint:* 16.8 min, 3.383 Ah, 0.1037 %, 51.8 %.

(b) Load scenario 4, Riding the limit, and run it as shipped. *Checkpoint:* 21.3 min, 0.000 Ah, 0.0780 %, 39.0 %.

(c) From the tiles, find the minutes the anode limit costs, the share of the fade it saves, and the capacity of a 200 Ah pack it saves over five hundred charges. Give the answers within 2 %. *Checkpoint:* 4.5 min, 25 % and 25.6 Ah.

9.8 App challenge · 8 min

Load scenario 8, The model is optimistic, which sets the Kinetic model error to 0.70 and the Thermistor offset to 0.3. Use the default seed, the speed 5 and runs of 25 min. Read the Plated, Time to target and Peak temperature tiles, which should match the answers in their last digit.

(a) Run it as shipped. *Checkpoint:* 2.237 Ah, 18.5 min, 34.7 °C.

(b) Set the Thermistor offset to 1.0, press Reset and run again. Then set it to 0.0, press Reset and run again. *Checkpoint:* 0.187 Ah at 1.0 and 3.422 Ah at 0.0.

(c) Explain the sign of the result, and say what it means for a project that fits a better thermistor to this vehicle. *Checkpoint:* A reading that is low makes the map believe a colder, more resistive anode.

9.9 App challenge · 9 min

Load the challenge, scenario 13, Ten minutes at the services. Use the default seed, the speed 10, and let each run go to the 45 min judgment without pausing (about 5 s of wall time). Read Time to target, Plated, Peak temperature and After 500 charges at 45 min. The tiles should match the answers in their last digit.

(a) Run it as loaded. *Checkpoint:* 21.6 min, 14.196 Ah, 28.0 °C, 62.6 %.

(b) Reload, reveal the suggested settings before Run, and run again. *Checkpoint:* 30.7 min, 0.024 Ah, 26.5 °C, 18.9 %.

(c) Reload, reveal the suggestion, set Cooling to Fixed flow with the Coolant flow at 20 %, and run again. Say whether the attempt passes and why the flow matters. *Checkpoint:* 34.7 min, 0.169 Ah, a fail on plating.

9.10 Application area · 3 min

The model is one equivalent cell scaled to the pack. A supplier proposes to ship this chapter's 15 mV margin, justified by Table 9.7, on a pack whose cells differ from one another by several percent in kinetic resistance.

(a) Which cell must the management system defend, and how does the spread change the margin? *Checkpoint:* The weakest cell, and the margin must cover the spread as well as the table error.

(b) State the specification sentence the table supports, in the form a design review would accept. *Checkpoint:* A tolerance to a named model error, not a safety factor.

9.11 Application area · 3 min

A charging network quotes its charge times from ten to eighty percent, and an automaker offers to warm the pack from the drivetrain on the way to the post.

(a) Use scenario 10 to explain why the network stops the quote at eighty percent. *Checkpoint:* The last twenty points take 21.8 min against 21.3 min for the first seventy.

(b) Use scenario 6 to state what preconditioning is worth on a 0 °C day. *Checkpoint:* 44.80 min from a 0 °C arrival against 27.40 min from 15 °C.

9.12 Review the agent · 5 min

An AI assistant reviewing scenario 12, Four limits, one QP, writes: "The anode-limited selector reaches 95 % in 38.4 min and the predictive controller in 41.6 min. The selector held every limit on its instruments, so the predictive controller wastes 3.2 min and should not be used on this pack." Find the flaw, and say how to check it in the app with the default seed, at the speed 10 with runs of 50 min.